Journal of Materials Chemistry B

ROYAL SOCIETY OF CHEMISTRY

REVIEW

View Article Online
View Journal | View Issue

Cite this: J. Mater. Chem. B, 2023, 11, 4153

Ferritin nanocages: a versatile platform for nanozyme design

Chunyu Wang,†[ab] Qiqi Liu,†[b] Xinglu Huang *[b] and Jie Zhuang*[a]

Nanozymes are a class of nanomaterials with enzyme-like activities and have attracted increasing attention due to their potential applications in biomedicine. However, nanozyme design incorporating the desired properties remains challenging. Natural or genetically engineered protein scaffolds, such as ferritin nanocages, have emerged as a promising platform for nanozyme design due to their unique protein structure, natural biomineralization capacity, self-assembly properties, and high biocompatibility. In this review, we highlight the intrinsic properties of ferritin nanocages, especially for nanozyme design. We also discuss the advantages of genetically engineered ferritin in the versatile design of nanozymes over natural ferritin. Additionally, we summarize the bioapplications of ferritin-based nanozymes based on their enzyme-mimicking activities. In this perspective, we mainly provide potential insights into the utilization of ferritin nanocages for nanozyme design.

Received 31st January 2023,
Accepted 11th April 2023

DOI: 10.1039/d3tb00192j

rsc.li/materials-b

1. Introduction

The catalytic functions of natural enzymes are critical in living organisms. However, natural enzymes have poor environmental stability and are easily denatured at extreme pH and temperature, which makes them difficult to prepare and preserve. To solve this problem, researchers have developed artificial enzymes that can mimic natural enzymes more effectively. Rapid development of nanotechnology and emergence of numerous nanomaterials provide new insight for artificial enzymes. Nanozymes are nanomaterials with intrinsic enzyme-like activities that can catalyze substrates and chemical reactions like natural enzymes, with similar reaction dynamics and catalytic mechanisms.[1] Since the discovery of peroxidase-like activity of Fe_3O_4 nanoparticles (NPs) in 2007,[2] nanozymes with various enzyme-like activities such as peroxidase (POD), oxidase (OXD), catalase (CAT) and superoxide dismutase (SOD) have been reported and widely used in biosensing,[3–5] antibacterial,[6] antioxidant,[7,8] and theranostics applications.[9–11] Despite the remarkable progress of nanozymes, their applications still face many issues. For example, the catalytic activities of nanozymes are size-dependent. Nanozymes with a smaller size typically show higher enzyme-like

[a] School of Medicine, Nankai University, Tianjin 300071, China. E-mail: zhuangj@nankai.edu.cn
[b] Key Laboratory of Bioactive Materials for the Ministry of Education, College of Life Sciences, State Key Laboratory of Medicinal Chemical Biology, and Frontiers Science Center for Cell Responses, Nankai University, Tianjin 300071, China. E-mail: huangxinglu@nankai.edu.cn
† C. Wang and Q. Liu contributed equally to this work.

Chunyu Wang

Chunyu Wang received her bachelor's degree in 2017 from Southwest University, China. She is now pursuing her master's degree under the supervision of Professor Xinglu Huang. Her main research interests are to construct multifunctional nanoplatforms based on ferritin nanocages and investigate their functions in neurodegenerative diseases.

Qiqi Liu

Qiqi Liu received her PhD degree in 2022 from Nankai University, China. She is currently undertaking her postdoctoral research under the guidance of Professor Xinglu Huang. Her scientific interests are focused on the biological barrier penetration and biological effects of functional nanomaterials based on protein engineering principles.

activities due to their larger surface area.[2] However, synthesizing size-controlled nanozymes is still challenging. Additionally, some specific targeting capabilities of nanozymes are also necessary for disease theranostics, but this is not practical because of the complex steps involved. Furthermore, the protein corona that forms on the nanozyme surface affects their *in vivo* fates, which can alter their distribution and delivery efficiency. In recent years, some biomacromolecules such as heat shock protein (HSP),[12] encapsulating proteins,[13] virus-like particles (VLPs), phage P22[14] and lumazine synthase[15] have been used as pre-organized scaffolds or templates for nanomaterial construction. However, their biomedical applications are hampered due to their limited controllability and functionality. To tackle these problems, designable ferritin nanocages have been introduced as a promising display platform of artificial enzymes. As a natural iron storage protein, the biomineralization ability of ferritin enables the synthesis of metal clusters and metal oxides with restricted size and ferritin efficiently reduces the protein corona formation. Human H-ferritin (FTn) can also naturally target tumors by binding with its receptor, transferrin receptor 1 (TfR1), which is highly expressed among various types of tumors. In addition, ferritin can be customized on demand *via* genetic or chemical techniques to give more functions to nanozymes. These properties allow broad applications of ferritin based nanozymes in tumor diagnosis and treatment. Collectively, ferritin nanocages combine the designable advantages of protein scaffolds with the catalytic activities of nanozymes, thus creating more possibilities for the design of multifunctional nanozymes.

A well-summarized review of ferritin nanozymes was previously reported by Jiang *et al.*[16] In this review, we will systemically provide in-depth insights and detailed mechanisms of ferritin nanocages. Based on the properties, we will highlight the benefits of genetically engineered ferritin nanocages and discuss their potential in nanozyme design. We will also provide an update on the relevant design and biomedical applications of ferritin nanozymes from the past three years. Through this overview (Fig. 1), we hope to clarify the potential of genetically engineered ferritin in serving as a nanozyme generator and provide insights for better nanozyme design.

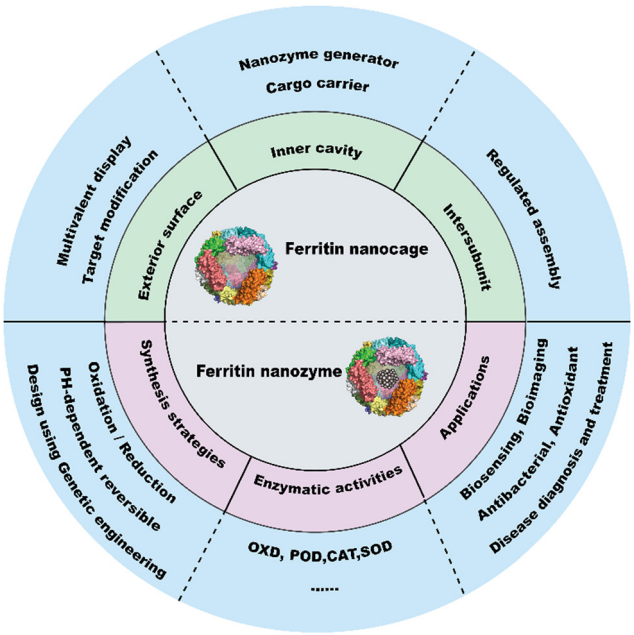

Fig. 1 Three designable interfaces of ferritin nanocages and ferritin as a nanozyme generator.

2. Ferritin nanocages as a multifunctional nanoplatform

2.1 Structure and function of ferritin

Ferritin was first discovered in horse spleen in 1937.[17] As a natural iron storage protein, ferritin is almost ubiquitous in

Xinglu Huang

Xinglu Huang obtained his PhD degree in 2010 from the Technical Institute of Physics and Chemistry at the Chinese Academy of Science. He then worked as a Postdoctoral Fellow at the National Institute of Health (NIH) and Johns Hopkins University (JHU). He is currently a Professor at Nankai University, China. His research focuses on the development of genetically engineered nanomedicines and AI-assisted nanotechnologies for exploring the interactions between nanomaterials and biological barriers, with aims to solve the problems facing oncology and regenerative medicine.

Jie Zhuang

Jie Zhuang obtained her PhD in 2010 from the Institute of Biophysics at the Chinese Academy of Sciences. After two years of postdoctoral training, she was promoted to Research Fellow at the National Institute of Health (NIH). She is currently an Associate Professor at the School of Medicine, Nankai University, China. Her research focuses on the development of protein-based nanozymes and their applications in the treatment of various diseases.

biological terms. To date, various species of ferritin have been identified, including bacteria, plants, animals, microorganisms, *etc.* Typically, ferritins are classified into three subfamilies, namely, classical ferritin (Ferritin), bacterial ferritin (Bfr), and DNA-binding proteins (Dps) from starved cells. Ferritin and Bfr proteins are classified as maxi-ferritin, consisting of 24 subunits that self-assemble to form a hollow cage-like structure with an inner and outer diameter of approximately 8 nm and 12 nm, respectively (Fig. 2a). Dps are classified as micro-ferritin with only 12 subunits, which are smaller than ferritin and Bfr.

Naturally, ferritin consists of a protein shell and an inner cavity. The inner cavity has a non-uniform ferric core composed of numerous iron hydroxide and phosphate molecules. Natural ferritin of different origins differs significantly in mineral core composition and structure. Bacterial and plant ferritin show higher phosphate ratios than mammalian ferritin, and the variation in phosphate causes different rates of iron mineralization for various types of ferritin.[18] The internal cavity of maxi-ferritin could accumulate up to 4500 iron atoms without affecting the normal function, which is crucial for maintaining iron homeostasis.[19,20] The properties of maxi-ferritin make it an ideal platform for nanomedicine, which will be mainly discussed in this review. Dps exhibit a lower iron storage capacity and a unique ferrous oxidase center.[21] It could also utilize H_2O_2 to rapidly oxidize Fe^{2+} to Fe^{3+} and store it in its inner cavity. Dps is a natural nanomaterial that can inhibit Fenton reactions and $^{\bullet}OH$ formation. Based on this, Min *et al.* introduced an appropriate amount of His into the N-terminal of the Dps to give it the function of cell membrane penetration. The modified Dps entered the cells *via* reticulin-mediated endocytosis and showed antioxidant effects on mouse dermatitis.[22]

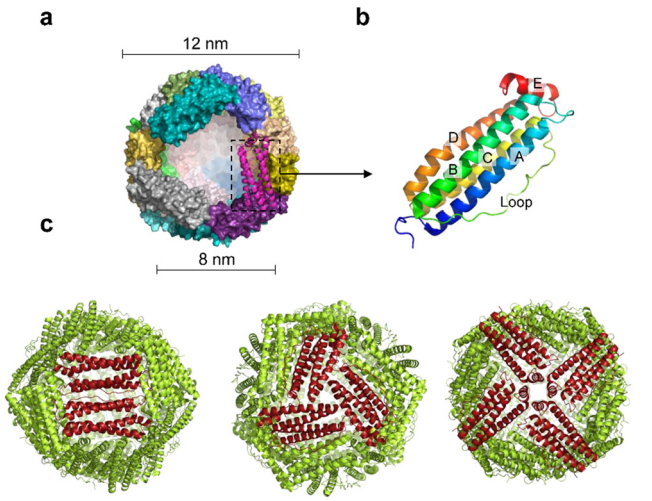

Fig. 2 Structure of ferritin nanocages. (a) A spherical cage-like structure composed of an iron core inside and a protein shell, with inner and outer diameters of 8 nm and 12 nm, respectively. (b) Four-helix bundle structure of a single subunit of ferritin. A, B, C, D: α-helix; E: short helix. (c) The tertiary structure of the human ferritin heavy chain presents 4.3.2 symmetry.

The amino acid sequences of ferritin from different species vary widely, but their spatial structure is highly conserved.[23,24] Specifically, each subunit of maxi-ferritin has four long α-helixes (A, B, C, D) from the N terminus, arranged in an antiparallel manner to form a helix bundle, and a short helix (E) forms the C terminus.[24] There are short non-helical regions at both N and C terminals as well as at the bends of AB and DE, while a long loop L is between B and C helixes (Fig. 2b). The 24 subunits form 12 pairs that are parallel and opposite to each other, creating a protein nanocage with 432 points of symmetry. There are 12 duplex, 8 triplex and 6 quadruplex axes/channels between ferritin subunits (Fig. 2c). Regarding the roles of these channels, ferritin with various electrostatic properties exhibit different functions. The C3 channel of mammalian ferritin is hydrophilic and contains six acidic amino acids, which allows metal ions and H_2O molecules to enter the ferritin cavity. However, based on the electrostatic properties of the bacterial ferritin (BfrA) of *Mycobacterium tuberculosis* (*Mtb*), it was demonstrated that the C4 channel and B-pore may be potential pathways for Fe^{2+} entry and play a role in Fe^{2+} uptake/oxidation in *Mtb* BfrA.[25] These channels of ferritin nanocages are critical for drug loading and nanozyme synthesis.

Mammalian ferritin, such as human ferritin, is composed of a H-subunit (21 kDa) and L-subunit (19 kDa). The H-subunit contains a ferroxidase site and the L-subunit has a nucleation site, both of which are essential for iron storage and distribution.[26] The ferroxidase site of the human H-subunit is mainly formed by three amino acid residues (Glu 27, Glu 62, His 65), which is important for maintaining ferroxidase activity.[27] Adjacent to the ferroxidase site are Glu residues on the inner surface of ferritin that facilitate iron core formation.[28] Mammalian ferritin occurs in different molecular forms called iso-ferritin with varying ratios of H and L-subunits. The H/L ratio depends on the proliferation, differentiation, and developmental stages of animal cells, which is consistent with the functions of ferritin. For example, ferritin in the heart and brain has a high H/L ratio with high ferroxidase activity for antioxidant function, which can efficiently oxidize and sequester iron. In contrast, ferritin in the liver and spleen has a low H/L ratio with high iron storage capacity.[20] Learning about the different H/L ratios of ferritin is important for understanding its structure and functions.

Besides the unique structure, ferritin also exhibits several natural functions. For example, ferritin nanocages could sequester excess cellular iron as hydrated iron oxide in their inner lumen, thus preventing oxidative damage caused by iron overload. It can also release iron to cells for synthesizing iron-containing proteins. The ferroxidase activity of ferritin is able to block the production of free radicals through the Fenton reaction. Furthermore, ferritin from different species exhibits distinct receptor binding properties, which are not fully understood. For instance, FTn could target tumors by recognizing the highly expressed TfR1 on the surface of tumor cells,[29,30] which makes it an ideal platform for active tumor targeting. However, the mouse H-ferritin is endocytosed by the TIM-2 (T-cell immunoglobulin and mucin structural domain protein 2) receptor.[31]

Regarding mouse L-ferritin, scavenger receptor class A member 5 (Scara5) has been identified as its receptor in the mouse kidney.[32] But human L-ferritin does not show a similar binding capacity to human Scara5. These natural receptor binding properties of various ferritins provide a reference for ferritin selection and practical applications.

2.2 Properties of natural ferritin

2.2.1 Biomineralization. In contrast to conventionally synthesized nanomaterials *in vitro*, ferritin is a natural biological nanomaterial generated by living organisms. Ferritin has the ability for iron biomineralization due to the high ferroxidase-like activity of its H-subunit, which also enables the encapsulation of metal NPs. For eukaryotic ferritin, the C3 pore plays an important role in Fe^{2+} sequestration.[33] The mechanisms of iron incorporation into ferritin *in vitro* can be described by four main steps: iron entry, iron oxidation, iron oxide nucleation, and iron oxide particle growth. This multistep mineralization process is mediated by the protein nanocage. Firstly, iron enters the cage through the C3 channel formed at the interface between subunits. Then the oxidation of Fe^{2+} is carried out through an enzymatic reaction at the ferroxidase center, resulting in the formation of Fe^{3+}. Next, after a series of complex hydrolytic reactions, the inner cavity of ferritin nanocages facilitates the nucleation of iron oxide particles with a confined size. During the Fe^{2+} sequestration process, the carboxylate side chains of Asp and Glu residues along the C3 pore (D127 and E130) are essential for iron uptake, while E136 and E57 (also known as translocation sites) play an important role in the transfer of Fe^{2+} from the C3 pore to the ferroxidase center.[34–37]

Besides selective Fe^{2+} sequestration, other metal ions could also be incorporated into ferritin nanocages under *in vitro* conditions.[34] For example, the X-ray crystal structure indicated that divalent metal ions, such as Cu^{2+}, Co^{2+}, Zn^{2+}, and Mn^{2+}, could bind to the C3 pore or ferroxidase center, thus competing with Fe^{2+} and reducing ferroxidase activity.[37–40] It was also revealed that His residues near the C4 pore could bind with Zn^{2+}, Cu^{2+}, Co^{2+}, Mn^{2+}, and Mg^{2+} to form octahedral geometry during Fe^{2+} sequestration in FTn and bullfrog M H-ferritin.[41] In horse spleen L-ferritin, Pd^{2+} could interact with H114, C126 and E130 and enter the ferritin nanocage through the C3 pore.[42] Moreover, the synthesis of Au NPs in ferritin has also been investigated in FTn, and Au^{3+} could interact with H65 and bind four His residues to form a square planar structure at the C4 pore.[43] Thus, different metal ions show different sequestration forms with various ferritin, which provides a reference for understanding and selecting ferritin nanoreactors for nanozyme synthesis. In fact, natural ferritin nanocages such as horse spleen ferritin (HosFt), human ferritin (HuFt), *Archaebacterial* ferritin (AfFt), and *Pyrococcus furiosus* ferritin (PfFn) have been widely used as a template for nanozyme synthesis. Under specific conditions *in vitro*, some metal NPs have been successfully assembled into ferritin to exert multiple functions, such as FeS, CdS, Mn_3O_4, and Fe_3O_4, *etc.*[44,45]

For the rational design and synthesis of ferritin nanozymes, it is important to understand how metal NPs grow in the ferritin cavity. The incorporation mechanism of NPs in ferritin is dependent on metal types and ferritin species, and it is not fully understood yet. Recently, several studies have shed light on this process. For example, the growth details of cobalt oxide NPs in ferritin nanocages were investigated by transmission electron microscopy (TEM) and the initial nucleation of small metals at the inner surface of ferritin was discovered.[46] The structural details of Pd ion accumulation in a ferritin nanocage were also revealed, which indicated that many metal ions could accumulate in the C3 channels of ferritin.[47,48] Therefore, the synthesis of metal NPs in ferritin may involve two steps: first, metal ions are pre-organized in the narrow channels of ferritin; second, they are converted into single sub-nanoclusters by oxidation or reduction reactions.[49,50] Moreover, the intermediate structures with flexible amino acid residues could be stabilized due to the unique coordination environment of the ferritin cavity,[51] thus resulting in the synthesis of metal NPs in a controlled manner.

2.2.2 Self-assembly of ferritin. Natural ferritin nanocages are self-assembled by 24 monomers to form a highly ordered structure, which allows the self-assembly forms to be modulated on demand. Specifically, various heterogeneous forms of ferritin nanocages could be obtained *via* modification of their subunits, which have new structures and functions compared to natural ferritin. For example, by altering the key subunit interface, Zhang *et al.* made progress in regulating the oligomerization state and structure of recombinant FTn. They inserted the peptide (∇139LNEQVKA) into the D-helix through a genetic strategy, which resulted in the transformation of the natural 24-polymeric ferritin nanocage into a lenticular 16-polymeric unnatural analogue.[52] Moreover, they constructed a 48-oligomeric ferritin nanocage by selectively deleting the amino acid residues at the key subunit interface (Δ139NEQVKA).[53] These novel designed ferritin nanocages help us better understand the self-assembly mechanisms of ferritin.

Natural ferritin maintains a stable cage-like structure over a wide pH range from 3.4 to 10.0, but when the pH of the solution is drastically and repeatedly changed, the structure undergoes the conversion between disassembly and reassembly. Under extremely acidic or alkaline conditions, the subunits depolymerize, and when the pH returns to neutral, the subunits reassemble into the nanocage.[54] However, the pH-induced disassembly and reassembly process is not fully reversible. When ferritin nanocages depolymerize at pH = 1.96, they could not recover to the original hollow spherical structure even after returning to neutral pH (Fig. 3).[55] Similarly, ferritin can disassemble under high concentrations of guanidine hydrochloride (6 M) and urea (8 M), and return to cage-like structures when these denaturing agents are withdrawn. Appropriate understanding of the *in vitro* self-assembly characteristics of natural ferritin is crucial for its applications in cargo loading, nanozyme synthesis and other biomedical fields. Several studies have reported the mechanisms of this process. Specifically, the self-assembly of ferritin is affected by multiple factors, such

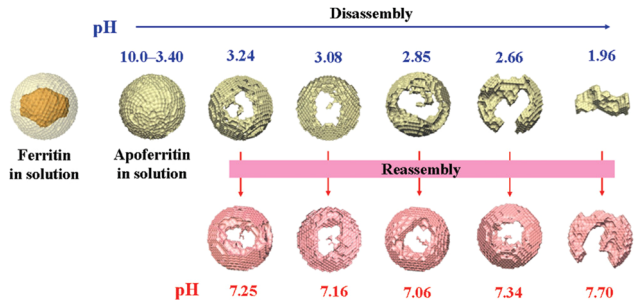

Fig. 3 The pH-induced apoferritin disassembly and reassembly processes.[55] Reprinted with permission from ref. 55, © American Chemical Society 2011.

as ferritin concentration, surface modifications, pH and ionic strength. For example, high concentrations of ferritin may promote unnecessary aggregation at lower pH and its surface modifications may affect subunit interactions.[56] Abhinav *et al.* used a laser scattering technique to study the self-assembly process of bullfrog M ferritin (BfMF, a structural and functional analogue of FTn).[57] It was found that the self-assembly kinetics of BfMF exhibited a unique manner. When the pH was increased from 1.5 to 7.0, the kinetic profile showed three phases: a rapid increase, a slow-down and a plateau. How different physical parameters affected the self-assembly process of BfMF was also investigated. For each individual factor, the rate of ferritin assembly increased with the concentration of protein, which was probably due to more opportunities for interactions caused by an increasing number of subunits. The rate of assembly decreased with the final pH of the solution. This was because the net negative charge strength of the ferritin subunits increased with pH, resulting in electrostatic repulsion between them, which explained the slow-down phase in the assembly kinetic profile. It was also found that the rate of assembly increased with the ionic strength (from 0.55 to 0.75 M), which was possibly due to the increased medium ionic strength that could shield the electrostatic repulsion between ferritin subunits. Also, as a multimeric protein cage, subunit–subunit interactions may be crucial for assembly.[58,59] A set of important His residues was shown to be involved in BfMF self-assembly, possibly by affecting the subunit–subunit interactions at the pore/interface due to its pH-dependent protonated/deprotonated state. It was reported that His also played an important role in regulating the reversible self-assembly of FTn.[60] Thus, understanding the self-assembly mechanisms of ferritin can help optimize the relevant parameters for incorporating nanomaterials into ferritin nanocages and provide insights into nanozyme synthesis.

2.3 Genetically engineered ferritin nanocages

The biomineralization and self-assembly properties of natural ferritin render it a powerful tool for nanomedicine design. However, natural ferritin nanocages need to be modified for more flexible and diverse functional applications. Recently, genetically recombinant ferritin nanocages have been developed to facilitate the diversification of ferritin design. In general, there are three functional interfaces of ferritin nanocages including the inner cavity, the outer surface, and the interface between subunits.[61] In particular, the 8 nm cavity provides a location for drug/biomacromolecules loading and nanozyme synthesis. For example, Zhang *et al.* have modified the electrostatics of ferritin to improve the loading efficiency of nucleic acid drugs. They replaced the negatively charged amino acids (Glu and Asp) on the internal surface of H-ferritin with positively charged ones (Lys and Arg) through genetic engineering.[62] Subsequently, these ferritin mutants with various electrostatics were screened and applied for efficient nucleic acid drug delivery.

Ferritin nanocage is an excellent display and delivery platform due to its easily modified outer surface. The N-terminus of ferritin is exposed on the outer surface of the nanocage, and various targeting peptides, antigens, and nanobody could be displayed onto ferritin *via* genetic or chemical methods. For example, the GRP78 targeting peptide SP94 was displayed on the outer surface of PfFn (named HccFn) by genetic engineering, and then Adriamycin (Dox) was encapsulated into the cavity of HccFn.[63] This nanomedicine (*i.e.*, HccFn–Dox) can be applied for targeted therapy of hepatocellular carcinoma. In detail, HccFn–Dox was bound to the glucose receptor binding protein (*i.e.*, GRP78) on the surface of hepatocellular carcinoma cells and was endocytosed. Then it localized in the lysosome, where the ferritin cleaved and released Dox in an acidic environment, thus leading to cell death.

Genetically recombinant FTn has attracted more attention in nanomedicine research in recent years. FTn preserves the optimal physicochemical properties and biocompatibility of natural ferritin, and it can specifically target tumor cells without further modification. These properties make FTn an ideal platform for cancer theranostics. For example, Liang *et al.* encapsulated large amounts of Dox into FTn to achieve effective tumor killing.[64] Fan *et al.* used FTn to synthesize Fe_3O_4 nanozymes for tumor targeting diagnosis.[65] More recently, our group synthesized multiple nanozymes in FTn for cancer treatment.[66–68]

2.4 Cargo carrier

The hollow spherical core of ferritin allows various cargo loading. To date, a variety of cargo molecules have been encapsulated into the cavities of ferritin nanocages, including drugs, imaging/contrast agents, nucleic acids, and metal NPs, and their applications cover the fields of bioassay analysis and various disease theranostics.[69] Table 1 summarizes the examples of drug or imaging/contrast molecules encapsulated in ferritin and their applications. Currently, the most common method for cargo loading is pH or urea dependent reassembly and disassembly. However, this method has some drawbacks. For example, extreme pH may damage the structure of protein cages and cargo molecules, thus reducing the encapsulation efficiency. It is desirable to explore more efficient ways for cargo loading in ferritin. Recently, Lin *et al.* reported that FTn had a natural hydrophilic drug entry channel and Dox could be encapsulated into its cavity by simple incubation at 60 °C for 4 h.[70]

Table 1 Examples of ferritin nanocages as cargo carriers

	Ferritin type	Molecules	Strategies	Applications	Ref.
Natural ferritin	HosFt	Desferrioxamine B	pH-dependent reversible assembly	None.	72
	HosFt	Cisplatin (CDDP) and carboplatin (CBDCA)	pH-dependent reversible assembly	MTT Test for drugs	73
	Genetically recombinant FTn	Curcumin	pH-dependent reversible assembly	Enhance the therapeutic effect of triple negative breast cancer	74
	Genetically recombinant FTn	Dox	Temperature control of drug channels	Prove the natural drug channel of ferritin heavy chain subunit	64,70
	Genetically recombinant FTn	CDDP	pH-dependent reversible assembly	Tumor targeted drug delivery and treatment	73
	Genetically recombinant FTn	Artesunate	Urea disassembly	Cooperate with internal ferric oxide to activate the anti-tumor effect	75
	Genetically recombinant FTn	MnPc	pH-dependent reversible assembly	Facilitate PDT in cancer	76
Genetically engineered ferritin	Genetically recombinant FTn	Metformin	pH-dependent reversible assembly	Targeted therapy for osteoarthritis	77
	Genetically recombinant FTn	Genz-644282	pH-dependent reversible assembly	Colorectal cancer targeted therapy	78
	Genetically recombinant FTn (point mutation)	TLR activating nucleic acid ligands	Construction of ferritin mutants with various electrostatics	Improved efficiency of TLR nucleic acid ligands delivery	79
	Genetically recombinant FTn	Paclitaxel (PTX)	Urea (20 mM) could expand the 4-fold channel size	Exhibited higher *in vivo* tumor therapeutic efficacy	80 and 81
	RGD4C-modified FTn	^{64}Cu, Cy5.5	pH-dependent reversible assembly	Multimodal imaging	82
	RGD4C-modified FTn	ZnF 16 Pc	Passive diffusion	Photosensitizer delivery, imaging, PDT	83

The encapsulation efficiency was up to 100 Dox molecules per protein, and the protein recovery reached more than 90%. Moreover, the FTn–Dox exhibited high stability, good safety and an excellent anti-tumor effect. In addition to Dox, Cisplatin (CDDP) and Oxaliplatin were also successfully loaded into the FTn *via* the channel. This strategy provided insights into the cargo loading in ferritin *via* a more convenient approach. Besides drug molecules, imaging signal molecules can also be incorporated into ferritin to construct a ferritin-based multifunctional nanoplatform. For example, Huang *et al.* loaded the NIR dye IR820 into ferritin to develop a novel therapeutic diagnostic probe for fluorescence imaging-guided photothermal therapy with high imaging contrast and enhanced photothermal conversion efficiency.[71]

2.5 Multivalent display platform

Ferritin nanocages are ideal carriers for antigen and peptide display due to their highly uniform size, symmetry, self-assembled repetitive structure and easily modified outer surface. Based on this, Zhang *et al.* designed a ferritin-based detection probe to improve the sensitivity of autoimmune disease detection.[84] Taking advantage of the multimeric display ability of ferritin, the antigen M3 and α-fodrin was arranged on the surface of ferritin, which greatly enhanced their ability to capture autoantibodies. In a similar manner, they developed a multimeric secondary antibody by displaying a human IgG binding peptide on the surface of ferritin and labeling it with Horseradish Peroxidase (HRP). This ferritin nanocage-based probe exhibited a higher affinity for human IgG, and its sensitivity was 10 times higher than conventional enzyme-labeled secondary antibodies. Combining the ferritin-based multimeric antigen with the secondary antibody probe, the sensitivity of human IgG detection was enhanced by 100–1000 fold. This ferritin-based capture system was an effective detection platform and created a new method for the diagnosis of autoimmune diseases. It also opened up more opportunities for ferritin as a multivalent display nanoplatform.

Ferritin nanocages also hold potential for vaccine design. In contrast to the weak binding of monovalent antigen, multivalent antigens displayed on a ferritin scaffold improve the recruitment of antigen presenting cells (APCs). The repeated arrangement of antigens also enables the effective activation of B cells. Ferritin vaccines have been a hot topic in new vaccine research due to the immunological and physicochemical properties, as well as the advantages of mass production through an *Escherichia coli* or eukaryotic system. Recently, Ma *et al.* developed a novel nanovaccine against SARS-Cov-2 by displaying the receptor binding domain (RBD) and heptapeptide repeat (HR) domain of spike protein onto ferritin *via* the Spy-Tag/Spy-Catcher system.[85] Compared to monomeric vaccine, this ferritin vaccine induced more potent neutralizing antibodies and cellular immune responses, which prompted novel vaccine design. Table 2 lists some examples of peptides or antigens displayed on the surface of ferritin.

3. Ferritin as a generator for nanozymes

3.1 Natural ferritin and genetically engineered ferritin for nanozyme synthesis

The biomineralization capacity and the size-constrained inner cavity of natural ferritin make it an ideal template for nanozyme synthesis. In 1991, Meldrum *et al.* used natural HosFt as a

Table 2 Examples of ferritin nanocages for antigen/peptide display

	Ferritin type	Antigen/peptide	Display strategies	Applications	Ref.
Natural ferritin	PfFn	M3, α-fodrin Fc binding peptide	N-Terminal fusion	Improve the sensitivity of ELISA for the diagnosis of autoimmune disease	84
	PfFn	SP94	N-Terminal fusion	Targeted therapy for hepatocellular carcinoma in combination with Dox	63 and 86
	PfFn	FcBP	D loop and E helix	Ability to bind the Fc region of antibodies	87
	PfFn	PreS1	N terminal	Hepatitis B virus vaccine	88
	Helicobacter pylori ferritin	GP140	N terminal	HIV-1 virus vaccine	89
	Helicobacter pylori ferritin	S protein	N Terminal	COVID-19 vaccine	85, 90 and 91
	Genetically recombinant FTn	EGF	N-Terminal fusion	Target breast cancer cells with high EGFR expression	92
	Genetically recombinant FTn	PAS and RGDK	N-Terminal fusion	PAS prolongs blood circulation time and RGDK increases tumor targeting	93
	Genetically recombinant FTn	BCP1	N-Terminal fusion	Enhance tumor therapeutic effect	94
	Genetically recombinant FTn	COL2	N-Terminal fusion	Targeted treatment of osteoarthritis with internal metformin	77
Genetically engineered ferritin	Genetically recombinant FTn	TNF Trimer	N-Terminal fusion	Mediate tumor cell apoptosis	95
	Genetically recombinant FTn	RGERPPR	C terminal	Combined with antitumor drug PTX, enhance therapeutic efficacy	80 and 96
	Human light chain ferritin	AP1 and RGD	157, N-terminal fusion	Super affinity and targeting to tumor cells	97 and 98
	Rat heavy chain ferritin	EV71 VP1 peptide	146/N terminal/C terminal	EV71 virus vaccine	99
	Helicobacter pylori ferritin (N19Q)	HA trimer protein	N terminal	Influenza virus vaccine	100–102

template to synthesize magnetic iron NPs in its cavity,[44] which started a new field of NP biosynthesis. Since then, multiple metal NPs such as Ag,[103] Au,[104] Pd,[105] Cu,[106] Co,[107] and Ni[108] have been incorporated into the cavity of HosFt. In addition, bacterial ferritin with high tolerance to harsh environments has also been discovered. For example, PfFn is an extremely thermally stable protein nanocage in which Pd–Ag NPs[109] and Co–Pt NPs[110] can be incorporated into its cavity. AfFt is another commonly used bacterial ferritin with a negatively charged inner surface and Au NPs can be loaded inside it.[111] Compared to other methods, the biomimetic synthesis of these ferritin nanozymes are characterized by the following features: (i) homogeneous particle size. The 8 nm cavity of ferritin provides a size-constrained template for nanozyme synthesis. (ii) Good biocompatibility and monodispersity. Ferritin is endogenous to an organism with low toxicity, immunogenicity and safe metabolites. (iii) Strong stability. Ferritin usually maintains structural stability over a wide range of temperature and pH. For some unstable nanozymes such as metallic NP materials, the overall stability can be improved by encapsulation of a ferritin scaffold. (iv) Simple synthesis. The NPs are easily synthesized inside ferritin nanocages at near room temperature and mild conditions. (v) Prolonged half-life *in vivo*. Rationally designed ferritin can exhibit prolonged blood circulation. For example, using a urea disassembly–reassembly approach, we prepared ferritin heterodimers *in vitro*,[112] which consist of H-chains and PEGylated H-chains of ferritin. Specifically, the H-chains provided TfR1 targeting to tumor cells and the PEGylated H-chains prolonged the circulation time *in vivo*. Furthermore, we constructed modularly assembled multimeric FTn-Ner nanostructures through PEG modification with various sizes, different morphologies and increasing binding valency to TfR1. These changes also led to differences in blood clearance of various ferritin oligomeric NPs. FTn-4er exhibited the best blood circulation half-life in mice, which facilitated the aggregation of ferritin nanozyme at the target site.[66]

Among various types of ferritin, it is necessary to choose the appropriate ferritin according to the biomedical applications of nanozymes. For example, for different species of ferritin, HosFt, AfFt and PfFt could better tolerate extreme environments, which might be suitable for *in vitro* assays and diagnostics. HuFt are ideal nanocarriers for disease treatments owing to their low immune responses induced by the body. Secondly, regarding natural and various modified ferritin, although natural ferritin can be used as simple templates for nanozyme synthesis, their applications are limited when certain targeting functions are required. Genetically and chemically modified ferritin nanocages could give nanozymes specific functions on demand. For example, recombinant FTn could recognize a TfR1 receptor more specifically with an enhanced tumor targeting ability. Moreover, the ferritin nanozyme was endowed with mitochondria-targeting abilities *via* tri-phenyl-phosphonium (TPP)-based modification.[113] Through gene fusion expression, SP94, a targeting peptide that specifically targeted hepatocellular carcinoma tissue, was incorporated into ferritin and the synthesized ferritin nanozyme could be applied for targeting

diagnosis of hepatocellular carcinoma samples.[86] It has been demonstrated that modification of the ferritin cavity *via* genetic engineering could improve the efficiency of metal NP synthesis. In detail, site-specific mutation of the inner lumen is beneficial for metal binding and growth, and the introduction of some specific components could facilitate the synthesis of metal NPs. For example, the synthesis of Ag NPs was achieved by doping silver-binding small peptides inside recombinant L-ferritin.[114] Likewise, the addition of Cys and His residues inside ferritin increased metal loading by sulfhydryl/imidazole chelation and enabled the synthesis of Au–Ag NPs.[43] The designable strengths of ferritin scaffolds combined with the catalytic activities of the nanozymes will fulfill more valuable applications in the future. Table 3 shows examples of ferritin-based nanozymes with various enzyme-like activities and their applications.

3.2 Strategies for the synthesis of ferritin nanozymes

The biomineralization process of iron in ferritin provides the theoretical basis for the synthesis of metal-based ferritin nanozymes. Due to the unique inner cavity and hydrophilic channels, metal ions could enter the ferritin easily and form a metal oxide core inside. Using ferritin as a protein scaffold, it is possible to synthesize size-homogeneous nanozymes in a controllable manner. At present, the most commonly used method for ferritin nanozyme synthesis is oxidation or reduction of metal ions in the ferritin cavity. To be specific, for the preparation of reductive nanozymes, different metal ions, such as Ir^{2+}, Pt^{2+}, Pd^{2+}, Cu^{2+}, Ru^{3+}, and Au^{2+} are incubated with ferritin under alkaline conditions (pH = 8.0), and these metal ions enter ferritin and form metal clusters *in situ* in the presence of the reducing agent $NaBH_4$. For oxidative ferritin nanozymes, such as Fe^{2+}, Mn^{2+}, and Co^{2+} are incubated with additional NaOH and oxidizing agent H_2O_2, which facilitate the formation of metal oxide NPs. In addition to *in situ* synthesis, metal NPs could also be loaded into ferritin nanocages *via* pH-induced disassembly and reassembly and the specific details have been discussed above. To sum up, these methods of nanozyme synthesis and the modification strategies of ferritin protein shells give rise to a ferritin nanozyme with diverse catalytic activities (POD, OXD, CAT, SOD, *etc.*) and biological functions.

Most relevant studies have focused on the formation of metal cores in the ferritin cavity. Indeed, structural analysis is also important to understand the coordination mechanisms and details of metal NPs in ferritin. X-ray crystal structure analysis has been used to observe how metal ions interact chemically inside protein crystals at different phases.[135,136] For example, Maity *et al.* used this method to show that Au ions moved toward the center of the C3 channels and formed sub-nanoclusters on ferritin. The amino acid residues that bound to Au ions changed the conformation of these sub-nanoclusters significantly.[137] Therefore, besides the metal–core form of ferritin nanozymes, metal moieties may also bind to other sites of ferritin such as C3/C4 channels, residues at key subunits and the outer surface, *etc.* More specific mechanisms and diverse designs of ferritin nanozymes will be explored in the future.

3.3 Biomedical applications of ferritin nanozymes with diverse catalytic activities

3.3.1 Ferritin nanozymes with POD-like activities. The POD-like activities of ferritin were first discovered in 1997 in HosFt.[138] Naturally, the intrinsic POD-like activities of ferritin could catalyze the decomposition of H_2O_2 to produce toxic $^{\bullet}OH$, which help regulate redox metabolism *in vivo*.[138–140] In 2011, Tang *et al.* demonstrated that HosFt could catalyze the oxidation of 3,3′,5′,5-tetramethylbenzidine (TMB), *ortho*-phenylenediamine (OPD), *etc.* at 50 °C, in the presence of H_2O_2. Moreover, even at high temperature (above 80 °C) or an extreme acidic environment (pH 2.0), it showed high POD-like activity, and its thermal stability and pH tolerance were comparable to that of HRP.[141] Recently, ferritin nanozymes with POD-like activities have been applied to kill tumor cell, virus and bacteria, *etc.* In addition, the generated $^{\bullet}OH$ can oxidize various dyes for biomolecular detection/sensing.

For disease-targeted catalytic diagnosis. The ferritin protein shell can interact with TfR1 and provide a natural binding scaffold, while the nanozyme core can provide a catalytic effect. In 2012, Fan *et al.* synthesized Fe_3O_4 NPs inside FTn with POD-like activities and tumor targeting abilities (M-FTn), which could catalyze the oxidation of substrate in the presence of H_2O_2 and result in a color reaction that visualized tumor tissue.[119] This study showed the potential of ferritin nanozymes for targeted diagnostic applications without any targeting ligands. Recently, they also found that the POD-like activities of M-FTn based nanozymes could identify and visualize macrophages in plaque samples from patients with a symptomatic carotid artery,[11] which expanded the application scopes of ferritin nanozymes.

Interestingly, except for metal NPs, hemin is the active site of POD and also has potential for biomimetic nanozyme design. However, hemin is hydrophobic and tends to aggregate, which makes it hard to control its structure and functions. Various materials such as polymers,[142] carbon nanotubes[143] and metal organic frameworks[144,145] have been used for hemin incorporation. Liu *et al.* used ferritin to encapsulate hemin and created a POD-like nanozyme (hemin@FTn),[122] which could target tumors and tolerate to harsh environments. Hemin@FTn could serve as a colorimetric probe for effective tumor cell detection. Although ferritin nanocages can target tumors by binding to TfR1, more diverse and accurate targeting modifications are urgent for a wider range of bioapplications. For instance, Jiang *et al.* designed a ferritin nanozyme with high POD-like activity and hepatocellular carcinoma targeting ability (HccFn–Co_3O_4).[86] The targeting peptide SP94 was modified on the outer surface of a ferritin nanocage *via* genetic fusion and Co_3O_4 was biomimetically synthesized in the inner cavity. HccFn–Co_3O_4 could specially target and visualize liver cancer tissues (Fig. 4), and its detection sensitivity was higher than that of the clinical marker α-fetoprotein (AFP). Taken together, the specific targeting ligands integrated into ferritin by genetic methods facilitate more precise and effective disease diagnosis.

Table 3 Examples of ferritin nanocages as nanozyme generators

Enzyme like activity		Ferritin type	Nanozyme core	Synthesis means	Applications	Ref.
POD	Natural ferritin	Horse spleen apoferritin	Au	Reduction	Glucose detection	115 and 116
		Horse spleen apoferritin	Prussian Blue NPs	Oxidation	Glucose detection	117 and 118
		PfFn	Co_3O_4	Oxidation	Hepatocellular carcinoma diagnosis	86
		Genetically recombinant FTn	Fe_3O_4	Oxidation	Tumor diagnosis	119
		Genetically recombinant FTn	Fe_3O_4	Oxidation	Pathological identification of ruptured atherosclerotic plaques	11
	Genetically engineered ferritin	Genetically recombinant FTn	Fe_3O_4	Oxidation	Modulate intracellular oxidative stress	120
		Genetically recombinant FTn	Pd	Reduction	Biorthogonal catalysis for targeted drug delivery	121
		Modular assembly FTn	Pt	Reduction	Prolong blood circulation and tumor accumulation	66
		Genetically recombinant FTn	Hemin	pH-dependent disassembly-reassembly	Tumor cell detection	122
CAT	Genetically engineered ferritin	Genetically recombinant FTn	Ru	Reduction	Enhanced tumor therapy	67
		Genetically recombinant FTn	$MnO_{2@}$Ce6	Oxidation	Enhanced effectiveness of tumor PDT	123
OXD	Natural ferritin	PfFn	Pd	Reduction	Catalyze the aerobic oxidation of alcohols	42
SOD	Natural ferritin	Horse spleen apoferritin	CeO_2	pH-dependent disassembly-reassembly	ROS scavenger	124
	Natural ferritin	Horse spleen apoferritin	Pt	Reduction	ROS scavenger	125 and 126
POD, CAT	Genetically engineered ferritin	Genetically recombinant FTn (apo)	$MnO_{2@}$Dox	Oxidation	TME-responsive tumor therapy	127
		Genetically recombinant FTn	Fe_3O_4	Oxidation	Treatment of cerebral malaria	128
	Natural ferritin	Horse spleen apoferritin	Pt	Reduction	Reduce cellular oxidative stress	129
SOD, CAT	Genetically engineered ferritin	Horse spleen apoferritin	Au–Pt alloy NPs	Reduction	Eliminate intracellular ROS	130
		TPP-labeled FTn	MnO_2	Oxidation	Mitochondria targeting alleviated oxidative damage	113
SOD, CAT, POD	Natural ferritin	Horse spleen apoferritin	Au–Ag alloy NPs	Reduction	Cytoprotecting	131
SOD, CAT, POD, OXD	Genetically engineered ferritin	Genetically recombinant FTn	Nitrogen-doped Porous Carbon Nanospheres (N-PCNSs)	Chemical modification	Tumor treatment	10
	Natural ferritin	Apoferritin	Cu	pH-dependent disassembly-reassembly	Trigger cell autophagy dependent apoptosis	132
Others	Genetically engineered ferritin	Horse spleen apoferritin	Au	Reduction	Imaging of breast cancer cells	133
		Genetically recombinant FTn	Cu	Reduction	Catalyze NO release; biomimetic design for artificial hybrid nanocells	134
		Genetically recombinant FTn	Pd	Reduction	Biorthogonal catalysis targeted drug delivery	121

For cancer-targeted catalytic therapy. FTn with tumor targeting abilities could make nanozymes more effective for catalytic therapy. Recently, our group introduced a fully synthetic cellular system based on POD-like ferritin nanozyme. Specifically, Fe_3O_4 NPs were *in situ* synthesized inside FTn and then they were integrated into membrane-mimicking vesicles, which could simulate the cellular oxidative stress process *via* a Fenton reaction[120] (Fig. 5). Moreover, this system could be delivered to tumor cells *in vivo* and catalyze H_2O_2 into toxic $^{\bullet}OH$ in the tumor microenvironment (TME), thus triggering tumor cell apoptosis and achieving tumor catalytic therapy.

In addition to the tumor targeting capability, our group also used ferritin nanocages to investigate the interactions between biomaterials and organisms on a nanoscale, which was also crucial for the biomimetic synthesis of nanozyme. Based on the concept of synthetic biology, we developed a modular assembly

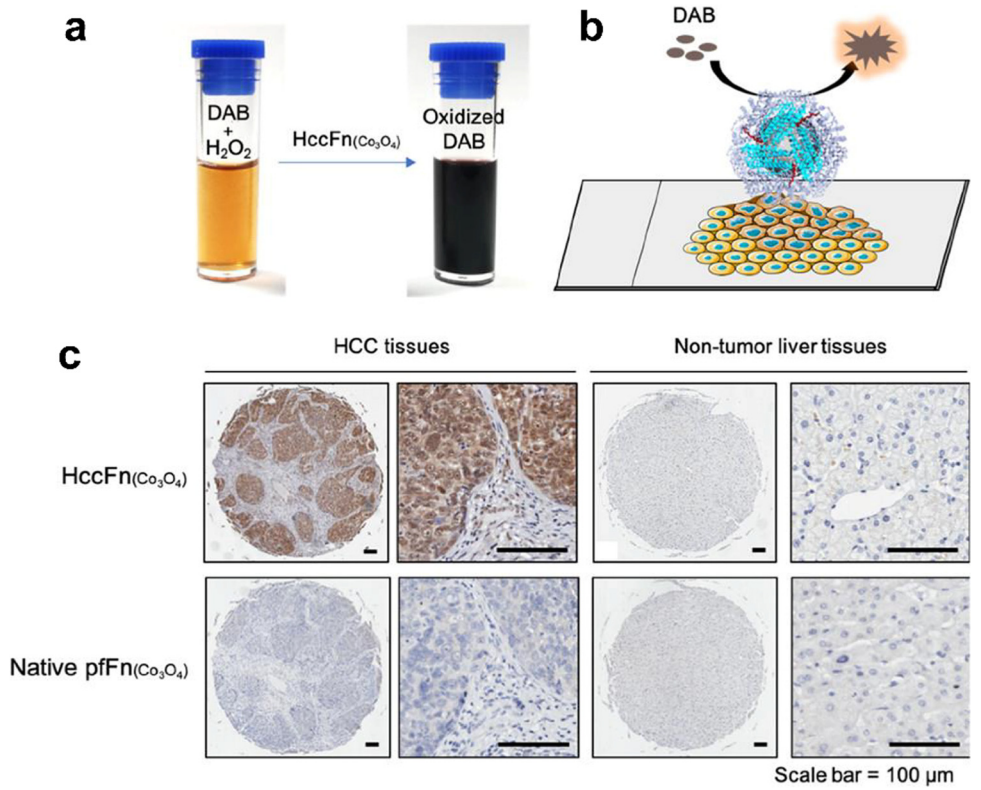

Fig. 4 HccFn (Co_3O_4) for the diagnosis of clinical HCC tissues.[86] (a) HccFn (Co_3O_4) nanozymes showed POD-like activity and catalyzed the oxidation of DAB to produce a colorimetric reaction. (b) Schematic diagram of the HccFn (Co_3O_4)-based IHC approach. (c) HccFn (Co_3O_4)-based IHC staining (top row) and native PfFn (Co_3O_4)-based IHC staining (bottom row) of HCC tissues and nontumor liver tissues. Reprinted with permission from ref. 86, © American Chemical Society 2019.

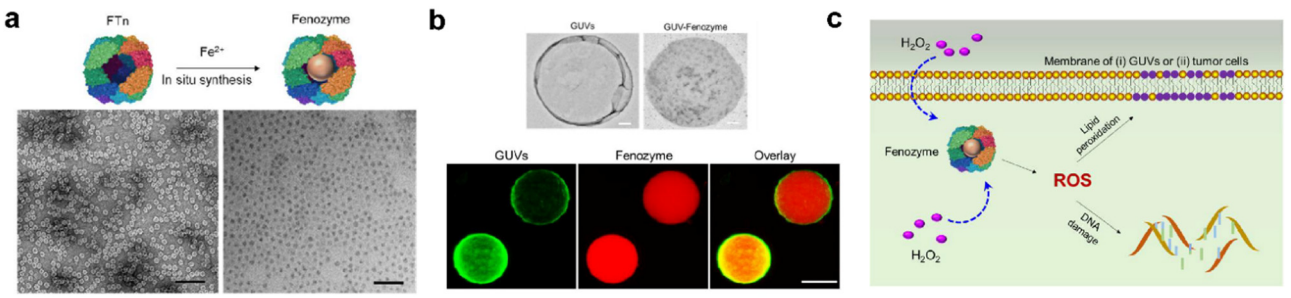

Fig. 5 Fenozyme-powered GUVs mimic oxidative stress in tumor cells.[120] (a) Fe_3O_4 NPs cores were *in situ* synthesized into FTn protein shells (Fenozyme). TEM image of Fenozyme loaded into GUVs. (b) Schematic illustration of Fenozyme packaged into GUVs using electroformation technology. (c) DNA damage mimicry and lipid peroxidation mimicry induced by GUV Fenozyme in tumor cells. Reprinted with permission from ref. 120, © American Chemical Society 2019.

strategy for precise and quantitative customization of highly ordered nanostructures.[66] Specifically, we used FTn as a protein building block, after recombination and purification in *Escherichia coli*, it was reassembled with PEG arms (Fig. 6a). Using the "bottom-up" hierarchical modular assembly idea, a series of nano multimers with ferritin nanocages were created (Fig. 6b). Then the Pt nanoclusters were incorporated into their cavities, which exhibited POD-like activity. As a result, these multivalent assembled ferritin nanozymes (FTn-Ner-Pt) with tunable protein structures and various binding domains were applied in tumor treatment. It was found that they could contribute to prolonged blood circulation time, effective accumulation in tumor cells *via* natural targeting abilities, and deep tumor issue penetration *via* a transcytosis mechanism, thus enhancing the anti-tumor efficiency (Fig. 6c and d). By integrating synthetic biology with nanotechnology, we offered a novel assembly strategy of ferritin nanocages, which opened up more possibilities for the *de novo* design of nanozymes.

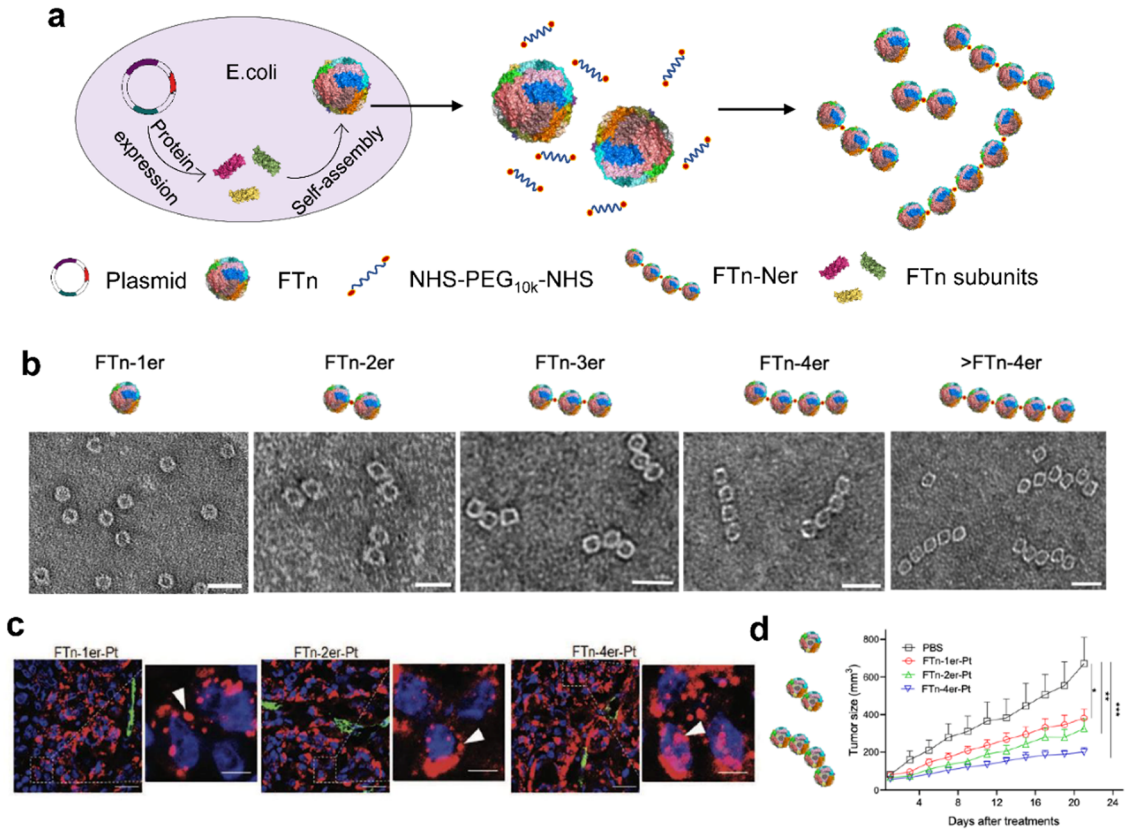

Fig. 6 Modular-assembly ferritin nanozymes.[66] (a) Schematic illustration for the preparation of FTn-Ner *via* a two-step self-assembly/post-assembly approach. The uniform FTn as motifs were obtained by the self-assembly of 24 FTn subunits expressed in *E. coli*. Subsequently, purified FTn motifs were further assembled to form different FTn-Ner by using two-armed PEG. (b) Representative TEM images of various assembled nanostructures. Scale bar: 20 nm (c) Representative confocal images of intracellular distribution of various Cy5-labeled FTn-Ner-Pt in HT29 tumor tissues 6 h following systemic administration. (d) Tumor growth curves of different groups of HT29 tumor-bearing mice after various indicated treatments. Reprinted with permission from ref. 66, © Wiley-VCH GmbH 2021.

3.3.2 Ferritin nanozymes with antioxidant enzyme-like activities

Ferritin nanozymes with SOD-like activities. Ferritin nanozymes with SOD-like activity can catalyze O^{2-} into O_2 and H_2O_2, which can serve as a ROS scavenger and antioxidant therapy. In 2012, nanoceria particles with a size of 4.5 nm were successfully encapsulated into the apoferritin through pH-induced disassembly and reassembly.[124] As a protein shell, the ferritin nanocage not only reduced the cytotoxicity of nano-CeO_2, but also modulated the electron localization at its surface, thereby enhancing the SOD-like activities of the nanozyme.

Ferritin nanozymes with CAT-like activities. Generally, the hypoxic microenvironment of malignant solid tumors hinders effective treatment, such as chemotherapy, radiation therapy, photodynamic therapy and acoustic dynamic therapy. Ferritin nanozymes with CAT-like activities could specifically target tumor tissue and catalyze the conversion of H_2O_2 into O_2 in a TME, which can act as a H_2O_2 scavenger for reducing oxidative stress and O_2 supplier for alleviating tumor hypoxia. Capitalizing on this, we synthesized MnO_2 NPs inside FTn to prepare a hypoxia-tropic nanozyme with CAT-like activity as an O_2 generator (OGzyme). Aggregation-induced emission (AIE) was also used as a photosensitizer for photodynamic therapy (PDT). The AIE molecules and OGzymes were encapsulated into phospholipid bilayers and the inner lumen of liposome, respectively, to develop a reaction cascade theranostic nanoplatform. Under light irradiation, the AIE molecules generated cytotoxic ROS, which also enabled imaging-guided PDT. The OGzymes supplied enough O_2 to relieve tumor hypoxia, and they were effectively enriched and penetrated in tumor tissues consequently. Thus, this cascade catalytic nanoplatform based on ferritin nanozyme enhanced PDT efficacy.[68] Veroniaina *et al.* designed a TME responsive nanozyme by encapsulating MnO_2 into FTn through oxidation. As a cargo carrier, Dox was also loaded inside FTn for combination therapy.[127] The hybrid MnO_2-Dox@FTn showed both POD and CAT activities which could produce abundant O_2 and Mn^{2+}, respectively, thus relieving tumor hypoxia and enabling MRI guided therapy. Zhu *et al.*[123] also synthesized MnO_2 in FTn and subsequently loaded Ce6, one of the most commonly used photosensitizers, to obtain an innovative therapeutic MnO_2-Ce6@FTn nanoplatform. This nanoplatform could accumulate in tumor tissues and catalyze the continuous production of O_2 from endogenous H_2O_2. Combining the advantages of

ferritin nanozyme with the photosensitizers Ce6, tumor PDT achieved great outcomes.

Moreover, nanozymes with different enzyme-like activities could be integrated in one platform to induce a cascade reaction for enhanced tumor therapy. Recently, our group utilized FTn as a nanozyme reactor for achieving enzymatic cascade reactions. We proposed a cascade catalytic nanoplatform using FTn as unique pre-coated protein corona and nanozymes as steady O_2 suppliers.[67] Specifically, ultra-small Au NPs were *in situ* synthesized into mesoporous silica nanoparticles (MSNs) which exhibited glucose oxidase-like activity. Then the Ru NP nanoclusters were encapsulated into the FTn inner cavity and showed CAT-like activity. The Au NPs catalyzed the oxidation of endogenous glucose to generate gluconic acid and H_2O_2, then FTn-Ru decomposed H_2O_2 into O_2 for alleviating hypoxia in a TME. Therefore, the cascade nanozymes achieved enhanced TME-responsive synergistic therapeutic outcomes. Taken together, the rational design of O_2-dependent therapies based on ferritin nanozymes has potential in tumor treatment.

3.3.3 Ferritin nanozymes with multienzyme-like activities. In recent years, an increasing number of nanozymes have been discovered to possess multiple enzymatic activities, which is also one of the most important features of nanozymes distinguishing them from natural enzymes. Multienzyme-like activities include: (i) nanozymes display different enzyme-like activities separately under different conditions; (ii) nanozymes exhibit two or more enzyme-like activities simultaneously under the same conditions. Due to the unique constrained inner cavity and other properties, ferritin nanocages have been demonstrated as an effective strategy for constructing a multienzyme cascade reaction system.

For cancer therapy. Due to the complex physiological environment *in vivo*, accurate and effective regulation of multienzyme activities of nanozymes remains challenging. In 2018, Fan *et al.*[10] reported a nitrogen-doped porous carbon nanozyme with four kinds of enzymatic activities (OXD, POD, CAT and SOD) to regulate ROS. Specifically, ferritin was used as a protein shell mediator to deliver nitrogen-doped porous carbon nanosphere nanozymes (N-PCNS) into lysosomes of tumor cells, which allowed the nanozymes to perform the required activities (Fig. 7). Under acidic conditions in lysosomes, the N-PCNS generated ROS to kill tumor cells through OXD and POD activities, while under a neutral environment, they exhibited CAT and SOD activities to scavenge free radicals, thus protecting normal cells from damage. Therefore, ferritin not only endowed N-PCNSs with the ability to target tumor cells, but facilitated the delivery of N-PCNSs to lysosomes where they initiated ROS production. This ferritin guiding N-PCNS showed

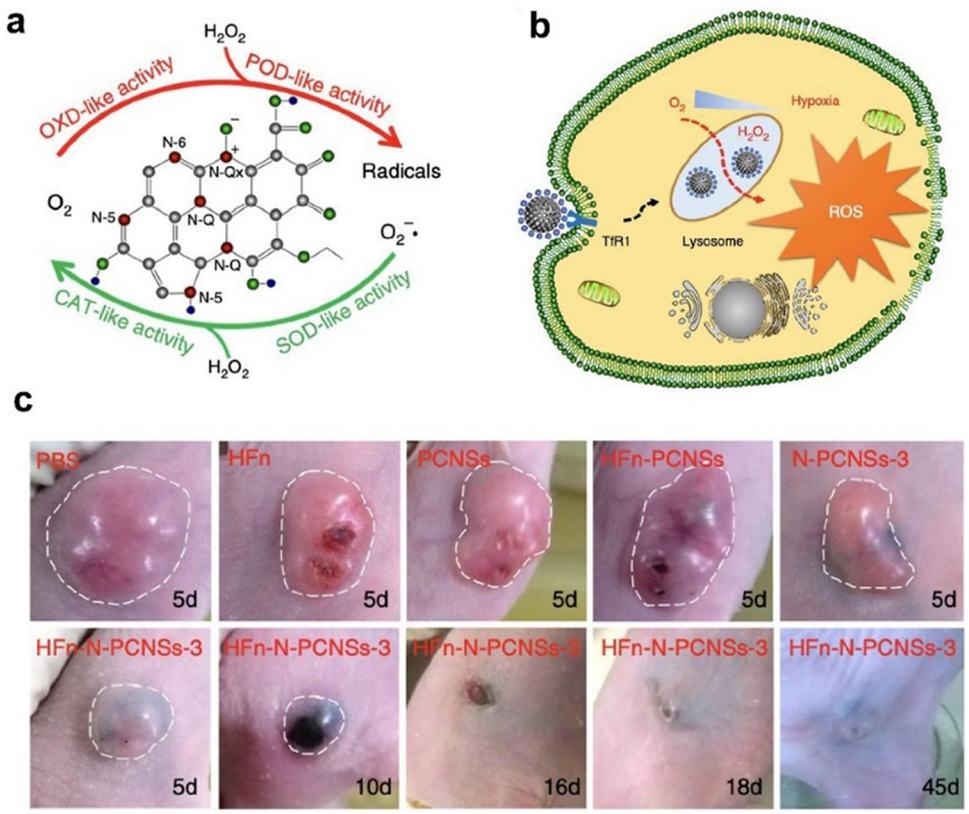

Fig. 7 Ferritin guiding N-PCNSs for cancer therapy.[10] (a) Schematic presentation of enzyme-like activities of N-PCNSs. (b) Schematic for N-PCNS induced tumor cell destruction *via* ferritin-mediated specific delivery. (c) Tumor morphology and progress with HFn-N-PCNSs treatment (n = 5). Reprinted with permission from ref. 10, © The Author(s) 2018.

multiple and controllable advantages for enhanced tumor therapy.

For cardiac ischemia-reperfusion injury alleviation. Based on *de novo* design of synthetic biology, we utilized FTn as the protein scaffold and synthesized MnO_2 in its inner cavity, then tri-phenyl-phosphonium (TPP) was modified onto the surface of ferritin nanocages *via* chemical methods for mitochondria targeting.[113] This novel ferritin Mn-SOD nanozyme (Mito-Fenozyme) was a promising joint cascade-catalytic platform, which exhibited high SOD-like and CAT-like activities. Moreover, this cascade nanozyme showed limited POD-like activities, thus protecting cells from toxic $^{\bullet}OH$. It was further confirmed that the Mito-Fenozyme could specifically target mitochondria and scavenge $^{\bullet}O_2^-$ to prevent mitochondrial oxidative injury through SOD-CAT cascade reactions (Fig. 8). We previously found that the receptors of ferritin were highly expressed under tissue hypoxia,[68,112,146] which enabled the Mito-Fenozyme to be delivered and enriched in the ischemic region. Taking advantage of our tailored ferritin nanozymes, we illustrated a combined therapeutic strategy for cardiac ischemia-reperfusion injury (IR) that integrated the targeting and catalytic capabilities of ferritin nanozymes, which could inspire further functional nanozyme design for other cardiovascular diseases.

For reconstruction of artificial cells. In addition to the significant effects and advantages in the treatment of various diseases, ferritin nanozymes have potential applications for mimicking artificial synthetic cells.[147] We have investigated the enzyme-mediated molecular mechanisms in artificial cells based on a ferritin nanozyme system. In particular, we synthesized eight metal nanozymes in FTn and screened them for various catalytic activities. Meanwhile, the corresponding inducers or inhibitors were also screened to modulate their enzyme activities. We constructed conceptual cell-mimicking catalytic vesicles based on ferritin nanozyme to simulate redox homeostasis events in living cells. We aimed to provide an example for the applications of ferritin nanozyme in the top-down construction of an artificial synthetic cellular system, which could expand the application fields of nanozymes.

3.3.4 Ferritin nanozymes with other enzymatic activities. Ferritin nanozymes also have other enzymatic activities for specific biological reactions besides the oxidoreductase activities. As we mentioned above, ferritin shows intrinsic ferroxidase-like activity, which is important for iron sequestration, antioxidant and detoxification metabolisms. Moreover, we constructed a FTn-based nanozyme library to better investigate their catalytic functions. It was unexpectedly found that FTn-Pd could mimic the activity of mutant $P450_{BM3}$ which cleaved the propargyl ether moiety specially. Also, FTn-Pd with intrinsic POD-like activity produced free radicals under acidic conditions, thus causing leakage of uncoated molecules from the lysosomal membrane to the cytoplasm. Therefore, we used FTn-Pd to achieve *in situ* bio-orthogonal catalysis and nanozyme-mediated lysosomal membrane leakage, which was successfully applied to model pro-drug design for anticancer therapy.[121]

Recently, we designed cell-like catalytic NPs based on FTn nanozyme and applied them to vascular regeneration in ischemic tissue (Fig. 9).[134] We found that copper-containing FTn nanozyme (FTn-Cu) enhanced the accumulation of NPs in ischemic tissues and promoted NO production from endogenous NO donor, such as *S*-nitrosothiol (R'SNO). Moreover, by mimicking biological processes, we previously demonstrated

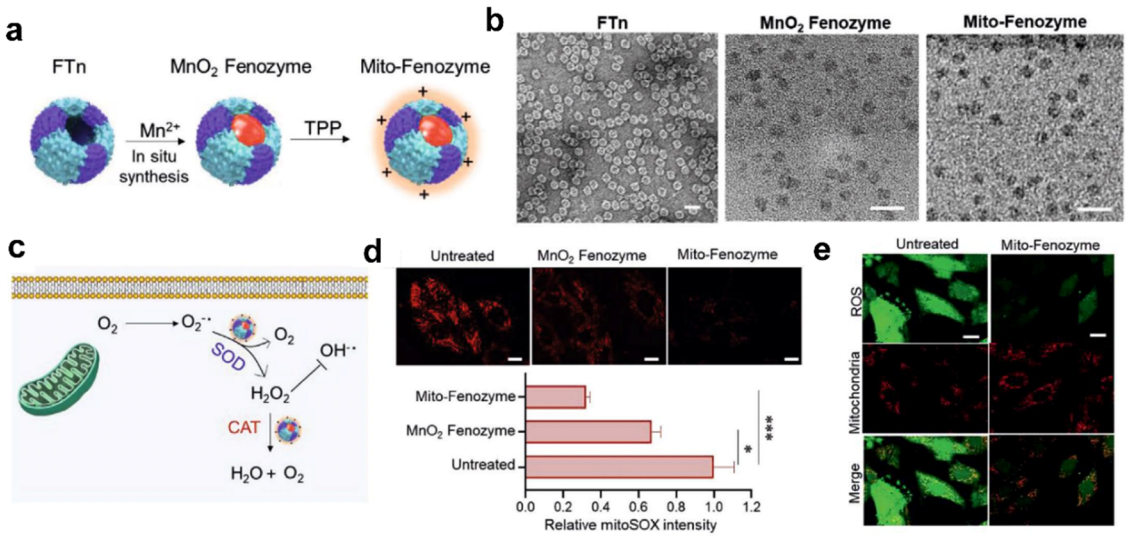

Fig. 8 Hybrid ferritin nanozyme (Mito-Fenozyme) protects mitochondrial functions.[113] (a) Schematic diagram for the preparation of Mito-Fenozyme. (b) TEM images of the FTn protein shell (negative staining with 1% uranyl acetate), MnO_2 NPs inside the FTn shell and Mito-Fenozyme. Scale bar: 20 nm. (c) Schematic diagram for the intracellular conversion of free radicals to non-cytotoxic molecules under the catalysis of Mito-Fenozyme. (d) Confocal images (top) and quantitative analysis (bottom) for the effect of Mito-Fenozyme on mitochondrial oxidative damage. (e) Mito-Fenozyme reduced intracellular free radical levels in oxidatively damaged cells. Reprinted with permission from ref. 113, © Wiley-VCH GmbH 2021.

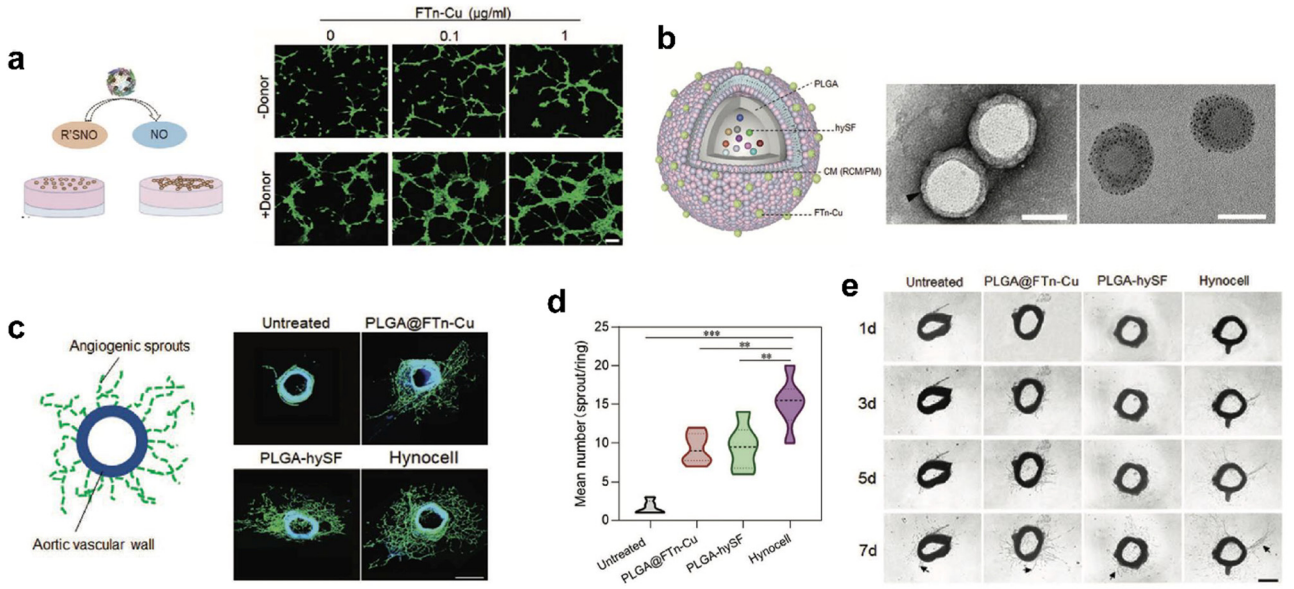

Fig. 9 Artificial Hynocell with FTn-Cu nanozyme for boosted vascular regeneration in ischemic tissues.[134] (a) Tube formation capacity of HUVECs with or without FTn-Cu treatments in the absence and presence of NO-donors. Scale bar: 100 μm. (b) Schematic illustration of the conceptual design of Hynocell. The Hynocell was prepared by loading hySF into PLGA, followed by coating with FTn-Cu fused CM (RCM and PM); TEM images of PLGA-CM-FTn after negative staining (left) and PLGA@FTn-Cu without negative staining (right). Scale bar: 100 nm. (c and d) Representative images and quantification analysis of induced sprouts of endothelial microvessels after different treatments based on an aortic ring assay at day 7. The formed capillary-like structures were stained with FITC-labeled phalloidin (green). Scale bar: 500 μm. (e) Representative images of microvessel sprouts (arrow) from *ex vivo* culture of mouse aortic rings in fibrin gel. Reprinted with permission from ref. 134, © Wiley-VCH GmbH 2022.

that bioactive factors secreted by hypoxic stem cells could promote angiogenesis effectively.[134] Based on this cellular mimicry, we constructed artificial hybrid nano-cells (Hynocell) by integrating hypoxic stem cell secretome into NPs with a cell membrane surface coating fused to FTn-Cu. Hynocell fused with different cell-derived components provided synergistic effects of targeting ischemic tissues and promoting vascular regeneration in acute hindlimb ischemia (HI) as well as acute myocardial infarction models (MI). This was an innovation of building biomimetic nano-cells with ferritin nanozymes, which boosted the development of cell-free therapy.

4. Perspective

Ferritin has emerged as an excellent and promising platform for nanozyme design due to its unique protein structure and intrinsic properties. Natural ferritin can be used as a template for nanozyme synthesis because of its mineralization ability. Genetically engineered ferritin as a protein scaffold provides more possibilities for nanozyme design than natural ferritin. For example, their inner surface can be genetically modified to improve the catalytic efficiency and substrate selectivity of nanozymes. The entry channels of ferritin can be regulated by mutation or deletion of amino acids at specific sites to achieve the pass-through of small molecules and metal ions.[25,34,35] Furthermore, genetic engineering enables the display of targeting peptides/ligands on the surface of ferritin, making the obtained nanozymes with targeting capability in a label-free manner. Many essential issues are pending for nanozyme research, such as low enzyme-mimicking activities and poor substrate selectivity. Despite the fascinating properties of ferritin nanozymes, their catalytic activities are much lower than that of natural enzymes, which is also the main challenge of other nanozymes. Learning from engineered metalloenzymes would be a recommended direction for the rational design of nanozymes. The metalloenzymes account for 40% of all enzymes. Typically, they contain a catalytic active site and a flexible binding pocket for the substrate, providing a design principle for developing nanozymes with high enzyme-mimicking activity and specific substrate recognition. Undoubtedly, genetically modified ferritin shows great potential in these aspects. For example, by using a genetic engineering approach, ferritin-based nanozymes containing at least 24 active sites and 24 substrate binding pockets might be obtained by rational design since a ferritin nanocage is composed of 24 assembled protein subunits.

Enzymes are essential for maintaining cell functions by catalyzing a series of reactions to mediate cell metabolism, which is the basis for designing nanozymes for disease therapy. In this regard, most studies focus on how to achieve high enzyme-mimicking activities at a comparable or superior level. In our opinion, the delivery efficiency and the activity-maintaining of nanozymes are of equal importance. Several aspects are discussed as follows: (i) delivery efficacy in disease sites. Consistent with other nanomedicines, targeted delivery of nanozymes in disease sites is essential for treatment. However, the readily formed protein corona greatly limits the delivery efficacy of nanozymes due to their nonspecific absorption with

protein in plasma. (ii) Intracellular locations. After cell uptake, the nanozymes tend to be trapped into lysosomes (~pH 5.0). However, pH determines the enzyme-mimicking activities of nanozymes. For example, the same nanozyme possesses POD-like activity under acid conditions but exhibits CAT-like activity at neutral pH. (iii) Activity-maintaining in disease sites. The enzyme-mimicking activities of nanozymes are detected and screened in solution *in vitro*, which is not consistent with the complex microenvironment *in vivo*. For example, the formed protein corona greatly reduces enzyme-mimicking activities by hindering the access of substrate to catalytic active sites. The trapped nanozymes in lysosomes also render their unexpected enzyme-like activities. As protein-based nanozymes, ferritin nanozymes undoubtedly have advantages in the delivery efficiency and the activity-maintaining over other conventional nanozymes. These properties were demonstrated in our recent reports.[66–68,112,146] For example, FTn nanocages actively bind with TfR1, which is highly expressed in hypoxic cells, such as tumor cells and the cells involved in ischemic tissues. The intrinsic properties render their direct targeted delivery without extra modification. Furthermore, ferritin-based nanozymes do not easily form protein corona due to the protection of their protein shell. Ferritin-based nanozymes capable of reducing lysosomal trapping can also be designed using a genetic engineering strategy. Future studies should continue to improve the properties of ferritin nanozymes (*e.g.* substrate binding, enzyme-mimicking activity) by combining with the design of ferritin structure in order to maximize their therapeutic potential.

Conflicts of interest

The authors declare no conflicts of interests.

Acknowledgements

We acknowledge the support from the National Natural Science Foundation of China (NSFC) (82072054, 32271448), the National Key Research and Development Program of China (2022YFA1105100), the Tianjin Synthetic Biotechnology Innovation Capacity Improvement Project (TSBICIP-KJGG-014-03), and the Nankai University Hundred Young Academic Leaders Program.

References

1 M. Liang and X. Yan, *Acc. Chem. Res.*, 2019, **52**, 2190–2200.
2 L. Gao, J. Zhuang, L. Nie, J. Zhang, Y. Zhang, N. Gu, T. Wang, J. Feng, D. Yang, S. Perrett and X. Yan, *Nat. Nanotechnol.*, 2007, **2**, 577–583.
3 X. Y. Wang, Y. H. Hu and H. Wei, *Inorg. Chem. Front.*, 2016, **3**, 41–60.
4 A. Pratsinis, G. A. Kelesidis, S. Zuercher, F. Krumeich, S. Bolisetty, R. Mezzenga, J. C. Leroux and G. A. Sotiriou, *ACS Nano*, 2017, **11**, 12210–12218.
5 H. Wei and E. Wang, *Anal. Chem.*, 2008, **80**, 2250–2254.
6 L. Q. Mei, S. Zhu, Y. P. Liu, W. Y. Yin, Z. J. Gu and Y. L. Zhao, *Chem. Eng. J.*, 2021, **418**, 129431.
7 Y. Chen, H. Zou, B. Yan, X. J. Wu, W. W. Cao, Y. H. Qian, L. Zheng and G. W. Yang, *Adv. Sci.*, 2022, **9**, 2103977.
8 H. Zhao, R. Zhang, X. Yan and K. Fan, *J. Mater. Chem. B*, 2021, **9**, 6939–6957.
9 D. M. Duan, K. L. Fan, D. X. Zhang, S. G. Tan, M. F. Liang, Y. Liu, J. L. Zhang, P. H. Zhang, W. Liu, X. G. Qiu, G. P. Kobinger, G. F. Gao and X. Y. Yan, *Biosens. Bioelectron.*, 2015, **74**, 134–141.
10 K. L. Fan, J. Q. Xi, L. Fan, P. X. Wang, C. H. Zhu, Y. Tang, X. D. Xu, M. M. Liang, B. Jiang, X. Y. Yan and L. Z. Gao, *Nat. Commun.*, 2018, **9**, 1440.
11 T. Wang, J. Y. He, D. M. Duan, B. Jiang, P. X. Wang, K. L. Fan, M. M. Liang and X. Y. Yan, *Nano Res.*, 2019, **12**, 863–868.
12 S. H. Choi, I. C. Kwon, K. Y. Hwang, I. S. Kim and H. J. Ahn, *Biomacromolecules*, 2011, **12**, 3099–3106.
13 H. Moon, J. Lee, J. Min and S. Kang, *Biomacromolecules*, 2014, **15**, 3794–3801.
14 E. J. Lee, N. K. Lee and I. S. Kim, *Adv. Drug Delivery Rev.*, 2016, **106**, 157–171.
15 J. Min, S. Kim, J. Lee and S. Kang, *RSC Adv.*, 2014, **4**, 48596–48600.
16 B. Jiang, L. Fang, K. Wu, X. Yan and K. Fan, *Theranostics*, 2020, **10**, 687–706.
17 V. Laufberger, *Bull. Soc. Chim. Biol.*, 1937, **19**, 1575–1582.
18 A. Parida, A. Mohanty, B. T. Kansara and R. K. Behera, *Inorg. Chem.*, 2020, **59**, 629–641.
19 E. C. Theil, *Adv. Enzymol. Relat. Areas Mol. Biol.*, 1990, **63**, 421–449.
20 P. M. Harrison and P. Arosio, *Biochim. Biophys. Acta*, 1996, **1275**, 161–203.
21 Y. Zhang and B. P. Orner, *Int. J. Mol. Sci.*, 2011, **12**, 5406–5421.
22 X. H. Min, T. Fang, L. L. Li, C. Q. Li, Z. P. Zhang, X. E. Zhang and F. Li, *Nanoscale*, 2020, **12**, 2340–2344.
23 E. C. Theil, R. K. Behera and T. Tosha, *Coord. Chem. Rev.*, 2013, **257**, 579–586.
24 E. C. Theil, *Annu. Rev. Biochem.*, 1987, **56**, 289–315.
25 A. Parida, A. Mohanty, R. K. Raut, I. Padhy and R. K. Behera, *Inorg. Chem.*, 2023, **62**, 178–191.
26 P. D. Hempstead, S. J. Yewdall, A. R. Fernie, D. M. Lawson, P. J. Artymiuk, D. W. Rice, G. C. Ford and P. M. Harrison, *J. Mol. Biol.*, 1997, **268**, 424–448.
27 D. M. Lawson, A. Treffry, P. J. Artymiuk, P. M. Harrison, S. J. Yewdall, A. Luzzago, G. Cesareni, S. Levi and P. Arosio, *FEBS Lett.*, 1989, **254**, 207–210.
28 V. J. Wade, S. Levi, P. Arosio, A. Treffry, P. M. Harrison and S. Mann, *J. Mol. Biol.*, 1991, **221**, 1443–1452.
29 T. R. Daniels, T. Delgado, J. A. Rodriguez, G. Helguera and M. L. Penichet, *Clin. Immunol.*, 2006, **121**, 144–158.
30 T. R. Daniels, T. Delgado, G. Helguera and M. L. Penichet, *Clin. Immunol.*, 2006, **121**, 159–176.
31 T. T. Chen, L. Li, D. H. Chung, C. D. C. Allen, S. V. Torti, F. M. Torti, J. G. Cyster, C. Y. Chen, F. M. Brodsky,

E. C. Niemi, M. C. Nakamura, W. E. Seaman and M. R. Daws, *J. Exp. Med.*, 2005, **202**, 955–965.
32 J. Y. Li, N. Paragas, R. M. Ned, A. D. Qiu, M. Viltard, T. Leete, I. R. Drexler, X. Chen, S. Sanna-Cherchi, F. Mohammed, D. Williams, C. S. Lin, K. M. Schmidt-Ott, N. C. Andrews and J. Barasch, *Dev. Cell*, 2009, **16**, 35–46.
33 A. Mohanty, A. Parida, R. K. Raut and R. K. Behera, *ACS Bio Med Chem Au*, 2022, **2**, 258–281.
34 R. K. Behera and E. C. Theil, *Proc. Natl. Acad. Sci. U. S. A.*, 2014, **111**, 7925–7930.
35 R. K. Behera, R. Torres, T. Tosha, J. M. Bradley, C. W. Goulding and E. C. Theil, *JBIC, J. Biol. Inorg. Chem.*, 2015, **20**, 957–969.
36 A. Treffry, E. R. Bauminger, D. Hechel, N. W. Hodson, I. Nowik, S. J. Yewdall and P. M. Harrison, *Biochem. J.*, 1993, **296**, 721–728.
37 T. Tosha, H.-L. Ng, O. Bhattasali, T. Alber and E. C. Theil, *J. Am. Chem. Soc.*, 2010, **132**, 14562–14569.
38 K. Honarmand Ebrahimi, P.-L. Hagedoorn and W. R. Hagen, *Chem. Rev.*, 2015, **115**, 295–326.
39 L. Toussaint, L. Bertrand, L. Hue, R. R. Crichton and J. P. Declercq, *J. Mol. Biol.*, 2007, **365**, 440–452.
40 R. R. Crichton and J. P. Declercq, *Biochim. Biophys. Acta*, 2010, **1800**, 706–718.
41 O. Kasyutich, A. Ilari, A. Fiorillo, D. Tatchev, A. Hoell and P. Ceci, *J. Am. Chem. Soc.*, 2010, **132**, 3621–3627.
42 S. Kanbak-Aksu, M. Nahid Hasan, W. R. Hagen, F. Hollmann, D. Sordi, R. A. Sheldon and I. W. Arends, *Chem. Commun.*, 2012, **48**, 5745–5747.
43 C. A. Butts, J. Swift, S. G. Kang, L. Di Costanzo, D. W. Christianson, J. G. Saven and I. J. Dmochowski, *Biochemistry*, 2008, **47**, 12729–12739.
44 F. C. Meldrum, V. J. Wade, D. L. Nimmo, B. R. Heywood and S. Mann, *Nature*, 1991, **349**, 684–687.
45 J. F. Hainfeld, *Proc. Natl. Acad. Sci. U. S. A.*, 1992, **89**, 11064–11068.
46 J. W. Kim, S. H. Choi, P. T. Lillehei, S. H. Chu, G. C. King and G. D. Watt, *Chem. Commun.*, 2005, 4101–4103, DOI: **10.1039/b505097a**.
47 T. Ueno, M. Abe, K. Hirata, S. Abe, M. Suzuki, N. Shimizu, M. Yamamoto, M. Takata and Y. Watanabe, *J. Am. Chem. Soc.*, 2009, **131**, 5094–5100.
48 S. Abe, T. Hikage, Y. Watanabe, S. Kitagawa and T. Ueno, *Inorg. Chem.*, 2010, **49**, 6967–6973.
49 S. Abe, J. Niemeyer, M. Abe, Y. Takezawa, T. Ueno, T. Hikage, G. Erker and Y. Watanabe, *J. Am. Chem. Soc.*, 2008, **130**, 10512–10514.
50 P. A. Sontz, J. B. Bailey, S. Aln and F. A. Tezcan, *J. Am. Chem. Soc.*, 2015, **137**, 11598–11601.
51 K. Zeth, S. Offermann, L. O. Essen and D. Oesterhelt, *Proc. Natl. Acad. Sci. U. S. A.*, 2004, **101**, 13780–13785.
52 S. L. Zhang, J. C. Zang, W. M. Wang, H. Chen, X. R. Zhang, F. D. Wang, H. F. Wang and G. H. Zhao, *Angew. Chem., Int. Ed.*, 2016, **55**, 16064–16070.
53 S. L. Zhang, J. C. Zang, X. R. Zhang, H. Chen, B. Mikami and G. H. Zhao, *ACS Nano*, 2016, **10**, 10382–10388.
54 S. Kang, L. M. Oltrogge, C. C. Broomell, L. O. Liepold, P. E. Prevelige, M. Young and T. Douglas, *J. Am. Chem. Soc.*, 2008, **130**, 16527–16529.
55 M. Kim, Y. Rho, K. S. Jin, B. Ahn, S. Jung, H. Kim and M. Ree, *Biomacromolecules*, 2011, **12**, 1629–1640.
56 D. Sato, H. Ohtomo, Y. Yamada, T. Hikima, A. Kurobe, K. Fujiwara and M. Ikeguchi, *Biochemistry*, 2016, **55**, 287–293.
57 A. Mohanty, K. Mithra, S. S. Jena and R. K. Behera, *Biomacromolecules*, 2021, **22**, 1389–1398.
58 R. R. Crichton and C. F. A. Bryce, *Biochem. J.*, 1973, **133**, 289–299.
59 D. J. E. Huard, K. M. Kane and F. A. Tezcan, *Nat. Chem. Biol.*, 2013, **9**, 169–176.
60 C. Gu, T. Zhang, C. Lv, Y. Liu, Y. Wang and G. Zhao, *ACS Nano*, 2020, **14**, 17080–17090.
61 M. Uchida, S. Kang, C. Reichhardt, K. Harlen and T. Douglas, *Biochim. Biophys. Acta*, 2010, **1800**, 834–845.
62 B. Zhang, X. Chen, G. Tang, R. Zhang, J. Li, G. Sun, X. Yan and K. Fan, *Nano Today*, 2022, **46**, 101564.
63 B. Jiang, R. Zhang, J. Zhang, Y. Hou, X. Chen, M. Zhou, X. Tian, C. Hao, K. Fan and X. Yan, *Theranostics*, 2019, **9**, 2167–2182.
64 M. Liang, K. Fan, M. Zhou, D. Duan, J. Zheng, D. Yang, J. Feng and X. Yan, *Proc. Natl. Acad. Sci. U. S. A.*, 2014, **111**, 14900–14905.
65 K. Fan, L. Gao and X. Yan, *Wiley Interdiscip. Rev.: Nanomed. Nanobiotechnol.*, 2013, **5**, 287–298.
66 Q. Liu, J. Tian, J. Liu, M. Zhu, Z. Gao, X. Hu, A. C. Midgley, J. Wu, X. Wang, D. Kong, J. Zhuang, J. Liu, X. Yan and X. Huang, *Adv. Mater.*, 2021, **33**, 2103128.
67 Z. J. Liu, Q. Q. Liu, H. Q. Zhang, X. Y. Zhang, J. Wu, Z. Y. Sun, M. S. Zhu, X. Y. Hu, T. Y. Qi, H. L. Kang, R. Chen, X. L. Huang and J. Zhuang, *Adv. Funct. Mater.*, 2022, **32**, 2208513.
68 F. Gao, J. Wu, H. Gao, X. Hu, L. Liu, A. C. Midgley, Q. Liu, Z. Sun, Y. Liu, D. Ding, Y. Wang, D. Kong and X. Huang, *Biomaterials*, 2020, **230**, 119635.
69 J. Zhang, D. Cheng, J. He, J. Hong, C. Yuan and M. Liang, *Nat. Protoc.*, 2021, **16**, 4878–4896.
70 B. Jiang, X. H. Chen, G. M. Sun, X. R. Chen, Y. F. Yin, Y. L. Jin, Q. Mi, L. Ma, Y. L. Yang, X. Y. Yan and K. L. Fan, *Nano Today*, 2020, **35**, 100948.
71 P. Huang, P. F. Rong, A. Jin, X. F. Yan, M. G. Zhang, J. Lin, H. Hu, Z. Wang, X. Y. Yue, W. W. Li, G. Niu, W. B. Zeng, W. Wang, K. C. Zhou and X. Y. Chen, *Adv. Mater.*, 2014, **26**, 6401–6408.
72 J. M. Dominguez-Vera, *J. Inorg. Biochem.*, 2004, **98**, 469–472.
73 Z. Yang, X. Wang, H. Diao, J. Zhang, H. Li, H. Sun and Z. Guo, *Chem. Commun.*, 2007, 3453–3455, DOI: **10.1039/b705326f**.
74 P. Ji, X. Wang, J. Yin, Y. Mou, H. Huang and Z. Ren, *Drug Delivery*, 2022, **29**, 986–996.
75 P. Ji, H. Huang, S. Yuan, L. Wang, S. Wang, Y. Chen, N. Feng, H. Veroniaina, Z. Wu, Z. Wu and X. Qi, *Adv. Healthcare Mater.*, 2019, **8**, e1900911.

76 X. Lin, Q. Wang, C. Gu, M. Li, K. Chen, P. Chen, Z. Tang, X. Liu, H. Pan, Z. Liu, R. Tang and S. Fan, *J. Am. Chem. Soc.*, 2020, **142**, 17543–17556.
77 Y. He, E. Ren, Z. Lu, H. Chen, Z. Qin, J. Wang, M. He, G. Liu, L. Zheng and J. Zhao, *Nanomedicine*, 2020, **28**, 102210.
78 E. Falvo, A. Arcovito, G. Conti, G. Cipolla, M. Pitea, V. Morea, V. Damiani, G. Sala, G. Fracasso and P. Ceci, *Pharmaceutics*, 2020, **12**, 992.
79 Z. L. Zhu, H. Y. Luo, T. Wang, C. H. Zhang, M. M. Liang, D. Q. Yang, M. H. Liu, W. W. Yu, Q. Bai, L. N. Wang and N. Sui, *Chem. Mater.*, 2022, **34**, 1356–1368.
80 R. Li, Y. Ma, Y. Dong, Z. Zhao, C. You, S. Huang, X. Li, F. Wang and Y. Zhang, *ACS Biomater. Sci. Eng.*, 2019, **5**, 6645–6654.
81 R. Yang, Y. Liu, D. Meng, Z. Chen, C. L. Blanchard and Z. Zhou, *J. Agric. Food Chem.*, 2017, **65**, 1410–1419.
82 X. Lin, J. Xie, G. Niu, F. Zhang, H. K. Gao, M. Yang, Q. M. Quan, M. A. Aronova, G. F. Zhang, S. Lee, R. Leaprnan and X. Y. Chen, *Nano Lett.*, 2011, **11**, 814–819.
83 Z. P. Zhen, W. Tang, C. L. Guo, H. M. Chen, X. Lin, G. Liu, B. W. Fei, X. Y. Chen, B. Q. Xu and J. Xie, *ACS Nano*, 2013, **7**, 6988–6996.
84 Y. Zhang, Y. Li, J. Zhang, X. Chen, R. Zhang, G. Sun, B. Jiang, K. Fan, Z. Li and X. Yan, *Small*, 2021, **17**, e2101655.
85 X. Ma, F. Zou, F. Yu, R. Li, Y. Yuan, Y. Zhang, X. Zhang, J. Deng, T. Chen, Z. Song, Y. Qiao, Y. Zhan, J. Liu, J. Zhang, X. Zhang, Z. Peng, Y. Li, Y. Lin, L. Liang, G. Wang, Y. Chen, Q. Chen, T. Pan, X. He and H. Zhang, *Immunity*, 2020, **53**, 1315–1330e1319.
86 B. Jiang, L. Yan, J. Zhang, M. Zhou, G. Shi, X. Tian, K. Fan, C. Hao and X. Yan, *ACS Appl. Mater. Interfaces*, 2019, **11**, 9747–9755.
87 H. J. Kang, Y. J. Kang, Y. M. Lee, H. H. Shin, S. J. Chung and S. Kang, *Biomaterials*, 2012, **33**, 5423–5430.
88 W. Wang, X. Zhou, Y. Bian, S. Wang, Q. Chai, Z. Guo, Z. Wang, P. Zhu, H. Peng, X. Yan, W. Li, Y. X. Fu and M. Zhu, *Nat. Nanotechnol.*, 2020, **15**, 406–416.
89 K. Sliepen, G. Ozorowski, J. Burger, T. van Montfort, M. Stunnenberg, I. Bontjer, C. LaBranche, D. Montefiori, J. Moore, A. Ward and R. Sanders, *JAIDS, J. Acquired Immune Defic. Syndr.*, 2016, **71**, 52.
90 U. Kalathiya, M. Padariya, R. Fahraeus, S. Chakraborti and T. R. Hupp, *Biomolecules*, 2021, **11**, 297.
91 A. E. Powell, K. M. Zhang, M. Sanyal, S. G. Tang, P. A. Weidenbacher, S. S. Li, T. D. Pham, J. E. Pak, W. Chiu and P. S. Kim, *ACS Cent. Sci.*, 2021, **7**, 183–199.
92 X. Li, L. H. Qiu, P. Zhu, X. Y. Tao, T. Imanaka, J. Zhao, Y. G. Huang, Y. P. Tu and X. N. Cao, *Small*, 2012, **8**, 2505–2514.
93 S. Yin, Y. Wang, B. Y. Zhang, Y. R. Qu, Y. D. Liu, S. Dai, Y. Zhang, Y. L. Wang and J. X. Bi, *Pharmaceutics*, 2021, **13**, 521.
94 P. P. Jin, R. Sha, Y. J. Zhang, L. Liu, Y. P. Bian, J. Qian, J. Y. Qian, J. Lin, N. Ishimwe, Y. Hu, W. B. Zhang, Y. C. Liu, S. H. Yin, L. Ren and L. P. Wen, *Nano Lett.*, 2019, **19**, 1467–1478.
95 M. Kih, E. J. Lee, N. K. Lee, Y. K. Kim, K. E. Lee, C. Jeong, Y. Yang, D. H. Kim and I. S. Kim, *Biomaterials*, 2018, **180**, 67–77.
96 Y. Ma, Y. Dong, X. Li, F. Wang and Y. Zhang, *ACS Appl. Bio Mater.*, 2021, **4**, 2654–2663.
97 S. Kim, J. O. Jeon, E. Jun, J. Jee, H. K. Jung, B. H. Lee, I. S. Kim and S. Kim, *Biomacromolecules*, 2016, **17**, 1150–1159.
98 J. O. Jeon, S. Kim, E. Choi, K. Shin, K. Cha, I. S. So, S. J. Kim, E. Jun, D. Kim, H. J. Ahn, B. H. Lee, S. H. Lee and I. S. Kim, *ACS Nano*, 2013, **7**, 7462–7471.
99 Z. T. Wang, L. F. Xu, H. Yu, P. Lv, Z. Lei, Y. Zeng, G. Liu and T. Cheng, *Biomater. Sci.*, 2019, **7**, 1794–1800.
100 M. Kanekiyo, C. J. Wei, H. M. Yassine, P. M. McTamney, J. C. Boyington, J. R. R. Whittle, S. S. Rao, W. P. Kong, L. S. Wang and G. J. Nabel, *Nature*, 2013, **499**, 102–106.
101 N. Darricarrere, S. Pougatcheva, X. C. Duan, R. S. Rudicell, T. H. Chou, J. DiNapoli, T. M. Ross, T. Alefantis, T. U. Vogel, H. Kleanthous, C. J. Wei and G. J. Nabel, *J. Virol.*, 2018, **92**, e01349-18.
102 H. G. Kelly, H. X. Tan, J. A. Juno, R. Esterbauer, Y. Ju, W. B. Jiang, V. C. Wimmer, B. C. Duckworth, J. R. Groom, F. Caruso, M. Kanekiyo, S. J. Kent and A. K. Wheatley, *Jci Insight*, 2020, **5**, e136653.
103 J. M. Dominguez-Vera, N. Galvez, P. Sanchez, A. J. Mota, S. Trasobares, J. C. Hernandez and J. J. Calvino, *Eur. J. Inorg. Chem.*, 2007, 4823–4826, DOI: **10.1002/ejic.200700606**.
104 L. Zhang, J. Swift, C. A. Butts, V. Yerubandi and I. J. Dmochowski, *J. Inorg. Biochem.*, 2007, **101**, 1719–1729.
105 T. Ueno, M. Suzuki, T. Goto, T. Matsumoto, K. Nagayama and Y. Watanabe, *Angew. Chem., Int. Ed.*, 2004, **43**, 2527–2530.
106 D. Ensign, M. Young and T. Douglas, *Inorg. Chem.*, 2004, **43**, 3441–3446.
107 T. Douglas and V. T. Stark, *Inorg. Chem.*, 2000, **39**, 1828–1830.
108 M. Okuda, K. Iwahori, I. Yamashita and H. Yoshimura, *Biotechnol. Bioeng.*, 2003, **84**, 187–194.
109 M. Peskova, L. Ilkovics, D. Hynek, S. Dostalova, E. M. Sanchez-Carnerero, M. Remes, Z. Heger and V. Pekarik, *J. Colloid Interface Sci.*, 2019, **537**, 20–27.
110 C. C. Jolley, M. Uchida, C. Reichhardt, R. Harrington, S. Kang, M. T. Klem, J. B. Parise and T. Douglas, *Chem. Mater.*, 2010, **22**, 4612–4618.
111 J. Swift, C. A. Butts, J. Cheung-Lau, V. Yerubandi and I. J. Dmochowski, *Langmuir*, 2009, **25**, 5219–5225.
112 X. Huang, J. Zhuang, S. W. Chung, B. Huang, G. Halpert, K. Negron, X. Sun, J. Yang, Y. Oh, P. M. Hwang, J. Hanes and J. S. Suk, *ACS Nano*, 2019, **13**, 236–247.
113 Y. Zhang, A. Khalique, X. Du, Z. Gao, J. Wu, X. Zhang, R. Zhang, Z. Sun, Q. Liu, Z. Xu, A. C. Midgley, L. Wang, X. Yan, J. Zhuang, D. Kong and X. Huang, *Adv. Mater.*, 2021, **33**, e2006570.
114 R. M. Kramer, C. Li, D. C. Carter, M. O. Stone and R. R. Naik, *J. Am. Chem. Soc.*, 2004, **126**, 13282–13286.

115 R. Fan, S. W. Chew, V. V. Cheong and B. P. Orner, *Small*, 2010, **6**, 1483–1487.
116 X. Jiang, C. Sun, Y. Guo, G. Nie and L. Xu, *Biosens. Bioelectron.*, 2015, **64**, 165–170.
117 N. Gálvez, P. Sánchez and J. M. Domínguez-Vera, *Dalton Trans.*, 2005, 2492–2494, DOI: **10.1039/B506290J**.
118 W. Zhang, Y. Zhang, Y. Chen, S. Li, N. Gu, S. Hu, Y. Sun, X. Chen and Q. Li, *J. Nanosci. Nanotechnol.*, 2013, **13**, 60–67.
119 K. Fan, C. Cao, Y. Pan, D. Lu, D. Yang, J. Feng, L. Song, M. Liang and X. Yan, *Nat. Nanotechnol.*, 2012, **7**, 459–464.
120 X. Hu, X. Wang, Q. Liu, J. Wu, H. Zhang, A. Khalique, Z. Sun, R. Chen, J. Wei, H. Li, D. Kong, J. Zhuang, X. Yan and X. Huang, *ACS Appl. Mater. Interfaces*, 2021, **13**, 21087–21096.
121 Z. Sun, Q. Liu, X. Wang, J. Wu, X. Hu, M. Liu, X. Zhang, Y. Wei, Z. Liu, H. Liu, R. Chen, F. Wang, A. C. Midgley, A. Li, X. Yan, Y. Wang, J. Zhuang and X. Huang, *Theranostics*, 2022, **12**, 1132–1147.
122 M. Liu, Y. Zhu, D. Jin, L. Li, J. Cheng and Y. Liu, *Inorg. Chem.*, 2021, **60**, 14515–14519.
123 Y. Zhu, D. Jin, M. Liu, Y. Dai, L. Li, X. Zheng, L. Wang, A. Shen, J. Yu, S. Wu, Y. Wu, K. Zhong, J. Cheng and Y. Liu, *Small*, 2022, **18**, e2200116.
124 X. Liu, W. Wei, Q. Yuan, X. Zhang, N. Li, Y. Du, G. Ma, C. Yan and D. Ma, *Chem. Commun.*, 2012, **48**, 3155–3157.
125 J. Fan, J. J. Yin, B. Ning, X. Wu, Y. Hu, M. Ferrari, G. J. Anderson, J. Wei, Y. Zhao and G. Nie, *Biomaterials*, 2011, **32**, 1611–1618.
126 A. Sennuga-Arowolo, J. Marwijk and C. Whiteley, *Nanotechnology*, 2011, **23**, 035102.
127 H. Veroniaina, Z. Wu and X. Qi, *J. Adv. Res.*, 2021, **33**, 201–213.
128 S. Zhao, H. Duan, Y. Yang, X. Yan and K. Fan, *Nano Lett.*, 2019, **19**, 8887–8895.
129 L. Zhang, L. Laug, W. Munchgesang, E. Pippel, U. Gosele, M. Brandsch and M. Knez, *Nano Lett.*, 2010, **10**, 219–223.
130 L. Zhang, W. Fischer, E. Pippel, G. Hause, M. Brandsch and M. Knez, *Small*, 2011, **7**, 1538–1541.
131 F. Dashtestani, H. Ghourchian and A. Najafi, *Mater. Sci. Eng., C*, 2019, **94**, 831–840.
132 K. Xiong, Y. Zhou, J. Karges, K. Du, J. Shen, M. Lin, F. Wei, J. Kou, Y. Chen, L. Ji and H. Chao, *ACS Appl. Mater. Interfaces*, 2021, **13**, 38959–38968.
133 T. N. Aslan, E. Asik, N. T. Guray and M. Volkan, *J. Biol. Inorg. Chem.*, 2020, **25**, 1139–1152.
134 X. Zhang, Y. Zhang, R. Zhang, X. Jiang, A. C. Midgley, Q. Liu, H. Kang, J. Wu, A. Khalique, M. Qian, D. An, J. Huang, L. Ou, Q. Zhao, J. Zhuang, X. Yan, D. Kong and X. Huang, *Adv. Mater.*, 2022, **34**, 2110352.
135 C. Cavazza, C. Bochot, P. Rousselot-Pailley, P. Carpentier, M. V. Cherrier, L. Martin, C. Marchi-Delapierre, J. C. Fontecilla-Camps and S. Menage, *Nat. Chem.*, 2010, **2**, 1069–1076.
136 R. Kubota, S. Tashiro, M. Shiro and M. Shionoya, *Nat. Chem.*, 2014, **6**, 913–918.
137 B. Maity, S. Abe and T. Ueno, *Nat. Commun.*, 2017, **8**, 14820.
138 G. S. Arapova, A. N. Eryomin and D. I. Metelitza, *Biochemistry*, 1997, **62**, 1415–1423.
139 G. S. Arapova, A. N. Eryomin and D. I. Metelitza, *Biochemistry*, 1998, **63**, 1191–1199.
140 V. Borelli, E. Trevisan, F. Vita, C. Bottin, M. Melato, C. Rizzardi and G. Zabucchi, *J. Toxicol. Environ. Health, Part A*, 2012, **75**, 603–623.
141 Z. Tang, H. Wu, Y. Zhang, Z. Li and Y. Lin, *Anal. Chem.*, 2011, **83**, 8611–8616.
142 J. Y. Guo, Y. T. Liu, J. Q. Zha, H. H. Han, Y. T. Chen and Z. F. Jia, *Polym. Chem.*, 2021, **12**, 858–866.
143 W. W. Wu, Q. Q. Wang, J. X. Chen, L. Huang, H. Zhang, K. Rong and S. J. Dong, *Nanoscale*, 2019, **11**, 12603–12609.
144 A. M. Alsharabasy, A. Pandit and P. Farras, *Adv. Mater.*, 2021, **33**, 2003883.
145 Y. Shu, J. Y. Chen, Z. Xu, D. Q. Jin, Q. Xu and X. Y. Hu, *J. Electroanal. Chem.*, 2019, **845**, 137–143.
146 X. Huang, J. Chisholm, J. Zhuang, Y. Xiao, G. Duncan, X. Chen, J. S. Suk and J. Hanes, *Proc. Natl. Acad. Sci. U. S. A.*, 2017, **114**, E6595–E6602.
147 J. Wu, Y. Wei, J. Lan, X. Hu, F. Gao, X. Zhang, Z. Gao, Q. Liu, Z. Sun, R. Chen, H. Zhao, K. Fan, X. Yan, J. Zhuang and X. Huang, *Small*, 2022, e2202145, DOI: **10.1002/smll.202202145**.

